INVISTIGATING THE EFFECT OF FORMULATION VARIABLES ON THE PREPARATION OF CHITOSAN-THEOPHYLLINE NANOCOMPOSITE USING QUALITY BY DESIGN

Prepared by

Noor Firas Aziz

Supervised by

Dr. Samer Hasan Hussein-Al-Ali

Co-Supervised by

Prof. /Dr. Mowafaq Mohammed Ghareeb

A Thesis
Submitted to Faculty of Pharmacy as a Partial Fulfillment of the Requirements for Master's Degree in Pharmaceutical Sciences

Faculty of Pharmacy
Isra University
August, 2020

جامعة الاسراء

نموذج تفويض

أنا نور فراس عزيز، أفوض جامعة الاسراء بتزويد نسخة من رسالتي للمكتبات أو المؤسسات أو الهيئات أو الاشخاص عن حسب التعليمات النافذة في الجامعة.

التوقيع: Nore

التاريخ: ٢/٩/٢٠٢٠

Isra University

Authorization From

I'm Noor Firas Aziz, authorize Al-Isra University to supply copies of my Thesis to libraries or establishments or individuals on request, according to Al-Isra University regulations.

Signature: Nore

Date: 2/9/2020

COMMITTEE DECISION

This Thesis (INVISTIGATING THE EFFECT OF FORMULATION VARIABLES ON THE PREPARATION OF CHITOSAN-THEOPHYLLINE NANOCOMPOSITE USING QUALITY BY DESIGN) was Successfully Defended and Approved on 23thAugust,2020.

Examination Committee	**Signature**
Dr. Samer Hasan Hussein-Al-Ali (Supervisor). Associate Professor of Nanosciences. Isra University, Faculty of Pharmacy.	
Prof.Dr. Mowafaq Mohammed Ghareeb (Co-Supervisor). Professor-PhD in pharmaceutical science. University of Baghdad, Faculty of Pharmacy.	
Dr. Eman Zmaily Dahmash (Internal Member). Assistant Professor of Pharmaceutics and Pharmaceutical Sciences. Isra University, Faculty of Pharmacy.	
Dr. Samer R. Abulateefeh (External Member). Professor-PhD in, Pharmaceutical Technology and Drug Delivery. The University of Jordan, Faculty of Pharmacy.	

Dedication

(Don’t stop until you are proud of yourself). With this in mind, I insisted on overcoming the difficulties and bearing to be that far away my family, as this work done, thanks to Allah who gives me determination to face difficulties and to succeed in passing them.

I dedicate this work to My Father , my beloved one and thank him, who wishes to see me as the best person in the world, My father who loves me for nothing ,I hope you are well in good health , because without you I would not be today with this academic distinction, may Allah keep you for me.

To my beautiful Mother, my companion, who take care for my feelings, and she prays that I will have success in everything I do in life, I hope you are well in good health, may Allah keep you for me.

To my brother, Ali, my friend, and my beloved one, who supports me, I hope for you high success, and may Allah protect you for me.

To my sister, Tabarak, the most beautiful girl in my eyes. She prays for me and cries every time I travel from Iraq to Jordan. Now I am beside you. The days of separation have ended, and I hope that we will stay together forever, my beloved sister.

To my son, my little boy, and my beloved brother, Hamza. may Allah keep you for me and I hope you will stay by my side, and I wish you high success.

To all my family, my grandparents, aunts, uncles and friends in Iraq (Ruba, Dalya, Aisha, Sama, Raya, Dina, Reyam, Noor, Ghufran, Lina, Ala'a, Nora, Hamsa, Ghofran). I love you all very much.

To Sarah Khalil, my sister, who supported me when I were away from my family and my country and who gave me motivation and encourages me throughout my bachelor and master study. You are among the beautiful things that Jordan has given me. I love you and may Allah keep you for me.

To Noor Abdul-Ghafour, the beautiful thing during the master’s period that you have become a friend and sister to me, thank you for your presence and your support for me, I hope you will stay my sister forever, I love you.

To Lina Marwan, my friend and sister, who supports me and gives me reassurance despite the distances between us. I hope to see you always successful, I love you, may Allah keep you for me my positive energy in the world.

To Maimouna Shaker, who, despite the bad incident that brought us together, but it was an opportunity to have a sister who loves me and wishes me well, I love you, may Allah keep you for me.

At the end, I thank all my friends in Jordan and everyone who was as a light source when I need that source of light.

Acknowledgment

To my doctor and my supervisor, **Dr. Samer Hussein-Al-Ali**, who was a good example for me during this work, he encouraged and taught me and never tired of teaching me, and stood by my side even in the days that I had low performance, I am very lucky because you are my supervisor.

To my co- supervisor, **Prof.Dr. Mowafaq Mohammed Ghareeb**, I am happy that you were my supervisor me during this work. Thank you very much for your cooperation with me despite the distance between the two countries (Iraq and Jordan).

To **Anwar**, my companion in this academic achievement and this thesis, who stood beside me taught me and encouraged me, every time when I felt a weak, thank you and love you.

To **Rasha**, my doctor and the lab supervisor, she gave me love and encouragement in the beginning of my study and taught me not to give up whatever happened and to face difficult days with a smile, she did not get bored with me every time I asked her about anything, thank you, love you

To all my doctors during my master's study, they were good examples and I thank them for teaching me and their love.

I would like to thank **Wadi Alrafidain Company for Pharmaceutical Products** located in Iraq, Baghdad, for their assistance to complete this work.

And I thank **Dr. Abdel-Hamid Abdel-Rahman Al-Salem, General Director of Samarra Drug Industry,** for grateful help in carrying out this research.

And I thank **Hikma Pharmaceutical Company**, located in Jordan, Sahab, for their assistance to complete this work.

INVISTIGATING THE EFFECT OF FORMULATION VARIABLES ON THE PREPARATION OF CHITOSAN-THEOPHYLLINE NANOCOMPOSITE USING QUALITY BY DESIGN

ABSTRACT

The aim of this study is to employ nanoparticles as drug carriers. The study involved the preparation of theophylline chitosan nanoparticles (THP-CSNPs) to overcome problem of theophylline frequent dose and improve properties. The THP-CSNPs samples were prepared using several amounts of CS (50, 75, 100 and 150 mg) and tripolyphosphate (TPP) at different amounts (25, 50, 75, 100, and 200 mg) and pH (4, 5, 6 and 6.5) with constant mass of THP at 100 mg. The produced nanocomposites were characterized by Fourier Transform Infrared (FTIR) and in vitro release. FTIR assessments were performed to estimate the functional group of THP loaded CS nanocomposites with any possible interaction. Full factorial design (Minitab 18) for the purpose of analyzing the results by using graphical analysis such as surface and contour plots, Pareto chart, main effect plots, normal probability plot of the residuals and residuals versus corresponding predicted values plots and interaction plots. The independent variable was (CS, TPP and pH) while loading efficiency, zeta potential and particle size are the dependent variables. Through experiments, we were able to obtain theophylline-chitosan nanocomposites of an acceptable size range and high specefication, which succeeded to carry and preserve the drug and provide prolonged release of THP from the nanocomposites.

LIST OF FIGURES

LIST OF TABLES

LIST OF ABREVIATIONS

CS	**Chitosan**
°C	**Celsius**
DLS	**Dynamic light scattering**
DSC	**Differential scanning calorimetry (DSC)**
FTIR	**Fourier Transform Infrared Spectroscopy**
LE	**Loading efficiency**
mg	**Milligram**
ml	**Milliliter**
min	**Minutes**
nm	**Nanometer**
PS	**Particle size**
pH	**Power of hydrogen**
PBS	**Phosphate buffer solution**
rpm	**Rounds per minute**
R	**Correlation of Coefficient**
R2	**Coefficient of Determination**
R-sq.	**Square**
R-sq. (adj.)	**Adjusted**
R-sq. (pred)	**Predicted**
THP	**Theophylline**
TPP	**Tripolyphosphate**
UV-vis	**Ultraviolet-visible spectrophotometer**
VIF	**Variance inflation factors**
ZP	**Zeta potential**

%	**Percentage**
λmax	**Lambda max**

CHAPTER ONE

INTRODUCTION

1.1) Background of the Study

Controlled delivery of drugs has shown a primary focus of research in pharmaceutical industry pharmacy due to their ability to reach to target organ (finiOprea, Nistor, Popa, Lupusoru, & Vasile, 2012). The controlled delivery system exhibits a pattern of drugs release, in which the concentration of drug remains in the therapeutic window for a long sufficient period of time, achieving prolonged physiological effect. Polymers have achieved successful applications in formulating controlled drug delivery systems (Naahidi et al., 2013). Their small size enable several advantages such as sustained release in GIT, better penetration, and excellent uptake of cells (Kawashima, 2001). Additionally, these nanoparticles are bio degradable and non-toxic to cells (Weber, Coester, Kreuter, & Langer, 2000). All of these advantages make them optimal candidates for enhancement of efficacy.

Nanoparticles have several advantages such as better *in vivo* stability, long-term capacity release, and the ability to permeate through tiny capillaries and body compartments (Yih & Al-Fandi, 2006). Furthermore, nanoparticles could enhance bioavailability, change its pharmacokinetic and bio distribution, and assist in sustained-release reservoirs formation (Herman et al., 1997).

The principal requirements for the delivery of a nanoparticle include: small sized (50-200 nm), having high loading capacity, slow dissociation *in vivo*, and optimized targeting to the desired tissue with limited absorption by other tissues. The development of formulations that can have these characteristics with consideration of

the cost and the simplicity of the design is crucial for effective delivery system (De Jong &Borm, 2008; Jeong et al., 2010).

Chitosan is N-deacetylated derivative of chitin which is a linear polysaccharide formed from randomly arranged deacetylated units of β-(1-4)-linked D-glucosamine along with acetylated units of N-acetyl-D-glucosamine. Chitosan is produced from the chitin collected from shrimps and other crustacean shells and reaction it with alkali sodium hydroxide (Hadwiger, 2013).

Theophylline: (dimethylxanthine) has been prescribed to manage pulmonary diseases for a long time. It was prescribed as a bronchodilator; however, the relatively high doses are connected with many adverse effects. Therefore, theophylline administration decreased and the preference of inhalation of B2-agonists increases. Recently, it has been proved to have anti-inflammatory impacts on asthma and chronic obstructive pulmonary disease (COPD) at lower concentrations (Barnes, 2013).

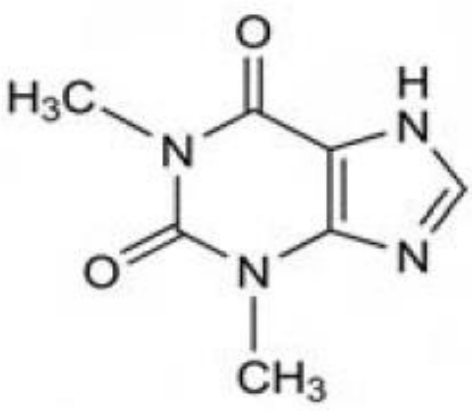

Figure 1.1 the structure of Theophylline

1.2) Physical-chemical properties of Theophylline

Theophylline is a natural alkaloid derivative of xanthine isolated from the plants *Camellia sinensis and Coffea arabica*. Theophylline inhibits phosphodiesterase and prostaglandin productions, regulate calcium flux, and antagonize adenosine. It has diuretic, smooth muscle relaxant, bronchial dilation, cardiac and central nervous system stimulant activities (Barnes, 2013).

Theophylline Chemical formula is C7H8N4O2 , Molecular mass 180.16 , pKa (basic)= 0.3 , pKa (acidic)= 8.6 , Melting point (ºC) 270-274 .It is slightly soluble (8.3 mg/ml) in water. It is soluble in 0.1 M HCl, 0.1 M NaOH and it is soluble in alcohol (12.5 mg/ml) (Andrei, 2011).

1.3) Problem Statement

Most drugs have some drawbacks such as poor stability, water insolubility, low selectivity, high toxicity, and adverse effects. Drug carriers should play a vital role in decreasing these problems. Nanoparticles composed of chitosan are drug carrier having the convenience of extended drug release which control solubility and stability of the drug, and can achieve enhancement of efficacy and reduction of toxicity (Shi, Fan, & Original, 2002).

The administration of drugs as a single dose rather than multiple doses has recently been made available using sustained release preparations. Prolonging the release of drug for a long period enables a constant level of the drug in blood. Theophylline (THP) is taken orally, intravenously, or as inhalation as an anti-asthma ((Zhao et al., 2015), (Feng et al., 2015)). However, recent researcher revealed that the dose range of THP which is optimized between efficacy and toxicity is narrow (i.e., therapeutic index of THP is between 10 to 20 μg/mL) (El-Sherbiny & Smyth, 2012). In addition, the short

half-life of THP may cause poor patient compliance due to frequent administration of the drug. Therefore, we used THP as a model drug to form THP-CS nanocomposites.

1.4) Design of Study

In the current study, the effect of three independent variables (CS, TPP and pH) on the three dependent variables (loading efficiency, zeta potential and particle size) was investigated using Minitab 18 software and different graphical analysis namely; contour, surface, main effects and interaction plots were performed. Degree of freedom (DF), adjusted sum of square (Adj SS), adjusted mean squares (Adj MS), P-value and Variance inflation factor (VIF) were used in the analysis.

1.5) Objectives

The aim of this research:

1. Optimization of theophylline loaded chitosan nanoparticles and studying the effect of different variables (tripolyphosphate, chitosan concentration, and pH value) on the loading efficiency, zeta potential, and particle size of nanocomposites.
2. Characterization of the optimized THP-CSNPs nanocomposites using FTIR.
3. Study *in vitro* theophylline release using PBS 7.4 from the selected nanocomposites formulation.
4. Novel research for experimental of design for theophylline-chitosan nanocomposites.

CHAPTER TWO

LITRETURE REVIEW

2.1) Nanoparticles Delivery Systems

The application of particulate delivery systems deserved further researchers care. Nanosized particles as a sort of particulate systems have been manipulated successfully as a recent approach of altering the pharmacodynamic and pharmacokinetic features of various drugs (Agnihotri, Mallikarjuna, & Aminabhavi, 2004).

Several polymers have been utilized in the formulation of nanoparticles to develop therapeutic compliance and decreasing adverse effects. The percent of drug entrapped into nanoparticles principally relying on how the formulation is done (Agnihotri et al., 2004).

The drug is reserved into a hole encircled with a unique film of polymer in nano-capsules while the drug which is entrapped in nanospheres is evenly dispersed (Mohanraj & Chen, 2006). In past years, biodegradable nanoparticles essentially those enclosed with hydrophilic polymers were employed as prospective carriers due to their capability of circulating for a longer period of time (Bhadra, Bhadra, Jain, & Jain, 2003).

2.2) Polymer Nanoparticles Preparation Methods

Polymeric nanosized particles were formulated usually by three principal approaches namely; preformed polymers dispersion, polymerization of monomers and ionic gelation (Reverchon & Adami, 2006). However, other techniques are applied too such as technology of supercritical fluid and particle replication in non-wetting templates and these are discussed in the literature for nanoparticles formulation (Rolland et al., 2005).

2.2.1 Dispersion of preformed polymers:

Preformed polymers dispersion is a familiar method which is manipulated to produce biodegradable nanoparticles from poly (D, L-glycolide), (PLG) , poly (lactic acid) (PLA), poly (cyanoacrylate) (PCA) and poly (D, L-lactide-co-glycolide) (PLGA) (Kompella, Bandi, & Ayalasomayajula, 2003). This technique can be applied in many ways including solvent evaporation emulsification or solvent diffusion techniques where both can be manipulated for either hydrophobic or hydrophilic drugs (Kompella et al., 2003).

2.2.2 Polymerization method*:*

In this method, monomers are polymerized to compose nanosized particles in an aqueous solution. The drug is incorporated either by being dissolved in the polymerization medium or by adsorption onto the nanoparticles after polymerization is completed (Ravi Kumar, Bakowsky, & Lehr, 2004).

2.2.3 Ionic gelation method*:*

Many researchers applied polymers for examples; gelatin, chitosan and sodium alginate as biodegradable hydrophilic polymers using different techniques. Among those a technique invented for hydrophilic chitosan nanoparticles preparation employing ionic gelation (Calvo, Remuñan-López, Vila-Jato, & Alonso, 1997). Ionic gelation method

requires a mixture of two aqueous phases one of them is chitosan as a polymer and the other is a poly-anion e.g. tripolyphosphate. In this case the positive charges of amino group of chitosan will interact with the negative charges of tripolyphosphate to compose nanocomposites (Calvo, RemuÞan-Lopez, Vila-Jato, & Alonso, 1997).

2.3) Polymer as Drug Delivery Carriers

Colloidal drug carriers such as polymer nanoparticle dispersions and micellar solutions liquid crystal consisting of microscopic particles of 10-400 nm in diameter show excellent candidate as drug delivery systems (Kramarenko, Khokhlov, & Reineker, 2006). In the formulation of those systems, the preference has been directed to optimize formulations with good drug loading and release characteristics with long expiry date and less toxicity. Although during formulation, the incorporation of drug sharing in the system structure might influence the interaction among molecules especially if the drug is amphiphilic and/or mesogenic (Kramarenko et al., 2006).

Nanoparticles could be of great advantage in the case of anticancer drugs to reduce its toxicity, increasing its bioavailability and efficacy. For example, Methoxy polyethylene glycol-block-Poly (D, L-lactide) (MPEG-PLA) was employed as a carrier in the formulation of lyophilized Deoxy-podophyllotoxin (DPT) loaded micelles. The formulated nanoparticles showed less cytotoxicity and had elevated clinical value, and could be considered to be a new antitumor preparation (Zu et al., 2020). Levodopa-loaded Poly (lactide-co-glycolide) nanoparticles were prepared to improve its bioavailability by overcoming excessive metabolism by aromatic amino acid decarboxylase in dopamine receptors for the nose to brain drug delivery. The effectiveness of the optimized nanoparticle formulation has been proved by in vivo studies (Arisoy et al., 2020).

For improving of targeting to the brain and bioavailability of nasal zolmitriptan, solid lipid nanoparticles (SLNs) gel for management of migraine, stearic acid and cholesterol were incorporated and lecithin as a surfactant. The optimized formula was prepared into HPMC gel to form nasal gel. histopathology of the tissues of brain proved that zolmitriptan nanoparticle nasal gel could reach brain and remained for 24 h (Dalia A. Elaty, Maha K. A, & Sameh. S, 2020).

Nanostructured Lipid Carriers (NLCs) composed of stearic acid: sesame oil mustard oil enriched with the powdered leaves extracts *Azadirachtaindica*(AE), *Lawsoniainermis*(LE) and fruit extract of *Mallotusphilippensis* (ME) were used in the treatment of psoriasis. The optimized batch of NLCs was found within the nanosized in diameter with zeta potential of-20mv and relatively low polydispersity index showing good encapsulation loading efficiencies. The in-vitro diffusion of drugs from the NLCs followed initial burst release then sustained release for 24 h (Kiran, Shadab, & Ghazala, 2020).

Eudragit S100 was used to formulate gliclazide (GLZ) nano sponges with increased bioavailability and sustained release. The GLZ nano sponge was prepared using various drug-polymer ratios (1:1 to 1:5). DSC and FTIR investigation indicate absence of interaction between drug and polymer. Evaluation parameters, proved that GLZ nano sponges could improve its bioavailability (SOLUNKE S.R., BORGE, MURTHY, DESHMUKH, & SHETE5, 2019).

Chitosan has gained a lot of interest as a polymeric drug carrier in many planned dosage forms, due to its properties such as biocompatibility, biodegradability, low toxicity, and its relatively low production cost as a result of its rich natural sources.

However, one disadvantage of using chitosan in modified release dosage forms for oral administration is the fast release rates that may happen in the stomach (Hamman, 2010).

Chitosan shows positive charge at low pH values which immediately joins negatively charged polyanions in solutions to develop CSNPs (Kean & Thanou, 2010).

Chitosan-nanpcomposites display favorable physicochemical characteristics with the maintenance of chitosan's biocompatible properties hence these complexes are considered to be useful excipients for the design of various kinds of dosage forms (Kean & Thanou, 2010).

2.4) Chitin and Chitosan

2.4.1 General information of chitin and chitosan

Due to their remarkable percent of nitrogen, 6.89% ,compared to artificial substituted cellulose (1.25%) chitin and chitosan are of commercial concern leading to harnessing chitin as a chelating agent. Natural polymers such as cellulose, chitin, chitosan and their derivatives have much more biocompatibility and biodegradability than most of the currently available synthetic polymers (Muzzarelli & Muzzarelli, 2005).

Existing in several places chitin is the fundamental component of arthropods such as insects, crustaceans, the beaks and internal shells of cephalopods squid and octopuses and in most invertebrates (Fabritius, Sachs, Triguero, & Raabe, 2009).

Chitin may be compared structurally with the polysaccharide cellulose in its high insolubility and its chemical reactivity. While functionally chitin could be compared to the protein keratin (Ravi Kumar, 2000).

Plain form of chitin is a white hard translucent and elastic substance while in its pure form it has a leathery texture. Albert Hofmann is the one who explained the chitin

structure in 1929 (Hofmann, 1929). Chemically chitin is a long-chain polymer of an N-acetylglucosamine (2-(acetylamino)-2-deoxy-D-glucose) a derivative of glucose (Shur, 2007). Chitin's N-acetylglucosamine units form covalent β-1, 4 linkages similar to the linkages among glucose units forming cellulose. This enables improved hydrogen bonding between neighboring polymers and increases the strength of chitin-polymer matrix. Chitin is commonly described as nitrogen-rich polysaccharide (Jain, Gupta, & Jain, 2007).

2.4.2 Synthesis of Chitosan from Chitin

Chitin is produced directly by physical and chemical processing of crustacean's shells; however, chitosan is synthesized from chitin. The chitin deacetylation by alkali is the traditional way for synthesis, whereas the alkali is sodium hydroxide (NaOH) is mostly used. The deacetylation is mainly determined by the alkali concentration, temperature, and time (Khor & Lim, 2003). Chitin is deacetylated in an excess amount of a NaOH solution as a reagent and water as a solvent at 1208 ˚C for 1-3 h in an oven for heating. Such treatment produces 70% deacetylated chitosan (Khor & Lim, 2003).

This reaction pathway, when complete deacetylation is allowed, produces about 98% deacetylated chitosan (Hu et al., 2002). The deacetylation process and the chemical modification of chitin and chitosan result in exposing the amino groups, which makes the molecule soluble in a majority of diluted acids and enhance their solubility in organic solvents (Mourya & Inamdar, 2008).The structures of cellulose, chitin, and chitosan are shown in **Figure 2.1**.

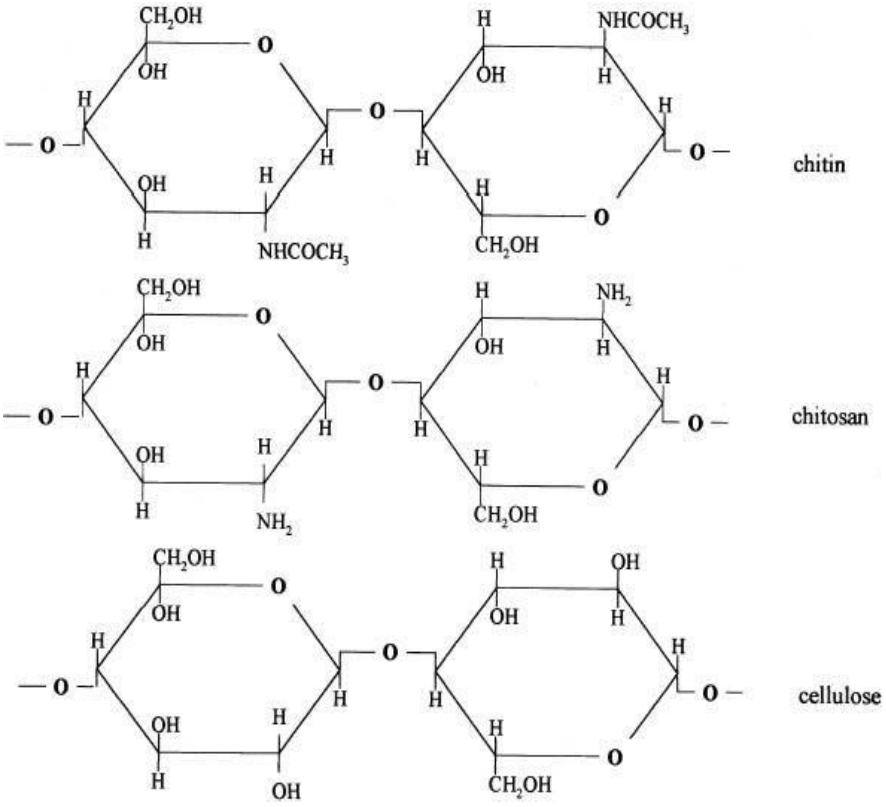

Figure 2.1 the chemical structures of chitin, chitosan and cellulose.

2.4.3 Applications of chitosan

Much attention has been paid to chitosan as a possible polysaccharide resource with many industrial and medical applications (Gupta & K., 2000). Chitosan is utilized currently in transdermal drug delivery and it is a suggested carrier in drug delivery systems. Chitosan has an antibacterial property and able to hinder the growth of *Fusarium, Alternaria, Escherichia coli, and Helminthophobia* (Wedmore, McManus, Pusateri, & Holcomb, 2006).

Lately, chitosan has been adopted as a gene carrier, the common virus has the drawbacks of low transfection rate and cell toxicity (Jayakumar et al., 2010). Chitosan has excellent biocompatibility and biodegradation, which has resulted in its popular applications. Furthermore, chitosan could be altered by folic acid to improve transfection efficiency. Folic acid could be easily absorbed by cells, improving the targeting of drugs. Mansouri et *al*., used folic acid to modify chitosan for improving gene transfection efficiency. They investigated systematically the properties of folic acid for gene treatment, proved that folic acid-modified chitosan nanoparticles had low cell toxicity, and could condense DNA effectively with ideal size and zeta potential. The results showed that folic acid-modified chitosan nanoparticles were a non-virus gene carrier with good application potential (Mansouri et al., 2006).

Protein drugs can be deteriorated easily by enzymes in vivo and have poor permeability and stability as well as a short half-life. Though, chitosan can preserve protein well and increase the contact between the drug and bio membrane so that improving bioavailability (Avadi et al., 2010).

Gan and Wang proved that altering the size and surface charge of chitosan–bovine serum albumin nanoparticles could regulate the encapsulation efficiency and release of

bovine serum albumin, but it was hard to control the burst release of protein of higher molecular weight (Gan & Wang, 2007).

Chitosan itself has particular antitumor activity and its positive charge could remove the negative charge on the tumor cell, producing selective absorption. Hence, chitosan nanoparticles can promote drug concentration in the tumor site and improve therapeutic efficacy. Doxorubicin/methoxy PEG grafted carboxymethyl chitosan nanoparticles with higher cell toxicity could enter cells and inhibit tumor-cell propagation efficiently (Jeong et al., 2010).

Paclitaxel (Taxol) derived from *Taxus brevifolia*, chitosan loaded nanoparticles were developed and employed for the treatment of several kinds of cancers. The researcher showed that the nanoparticle loaded drug exhibited better activity with sustained release, increased cell uptake, and lowered hemolysis compared with pure Paclitaxel (Gupta et al., 2017).

Formulated methylprednisolone containing chitosan-based nanoparticles using the ionic gelation. The selected formulation had a particle size of 243±2.33 nm with an efficiency of encapsulation of 79.3±7.2%. Morphology of the particles using SEM reveals nearly spherical shaped. Methylprednisolone showed prolonged release for about 24 h (Ganesh N, C. H. Praveen, Birendra, & B, 2020).

Controlled release nanoparticles gel of timolol maleate (TM) for treatment of infantile hemangioma by ionic gelation method using chitosan and sodium alginate. Calcium chloride (CaCl2) to produce the optimum formula of TM nanoparticles. Hydroxy Propyl Methyl Cellulose (HPMC) K15 was incorporated into optimum formula to prepare

nanoparticles gel of TM and carried out *in vivo* release study (Ahdyani, Novitasari, Martien, & Danarti, 2019).

Formulated and optimized simvastatin loaded chitosan-tripolyphosphate nanoparticles (SIM CS-TPP NPs) using ionic gelation method to provide a controlled release local delivery of simvastatin to promote bone regeneration. The ability of the optimum formula to stimulate bone regeneration upon implantation was evaluated. The optimum SIMCS-TPP NPs had particle size of 106 nm, zeta potential of 43.3 mv, polydispersity index of 0.295 and entrapment efficiency of 98.78% and also showed good storage stability (Delan et al., 2020).

2.5) Drug Release mechanisms

Maintaining the drug level in blood inside the therapeutic window in a steady-state between the minimum toxic concentration (MTC) and the minimum effective concentration (MEC) is considered the most crucial goal (Siegel & Rathbone, 2012). If a drug is taken as a single large dose, the level of drug may rise over MTC, generating adverse effects, and then quickly decreases below the MEC **(Figure 2.2).** Multiple doses with a particular interval may reduce the fluctuation but may meet patient non-compliance problems. Hence, it is helpful to afford drug carriers that provide prolonged release of a drug with low doses frequency. For this purpose, a continuous drug release rate (zero-order drug release profile) is often preferred (Bajpai, Shukla, Bhanu, & Kankane, 2008; Siegel & Rathbone, 2012).

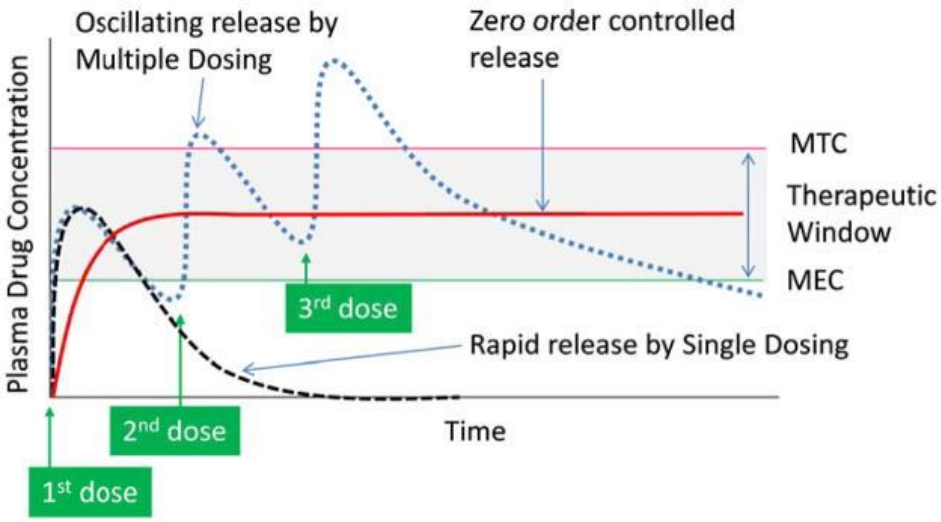

Figure 2.2 Plasma drug concentration of single dose (short dashed line), multiple dose (dotted line), and zero order-controlled release (solid line). The minimum toxic concentration (MTC) and the maximum effective concentration (MEC) (Lee & Yeo, 2015).

Several variables are influencing the release of drugs for example; the components (drug, polymer, and additives), proportion of each ingredient, interactions, and the preparation techniques. Concerning the drug release mechanism from a carrier, the release could be categorized into four classes (diffusion, stimuli controlled release, solvent, and chemical reaction) (Langer & Peppas, 1983; Siegel & Rathbone, 2012). As illustrated below **(Figure 2.3).**

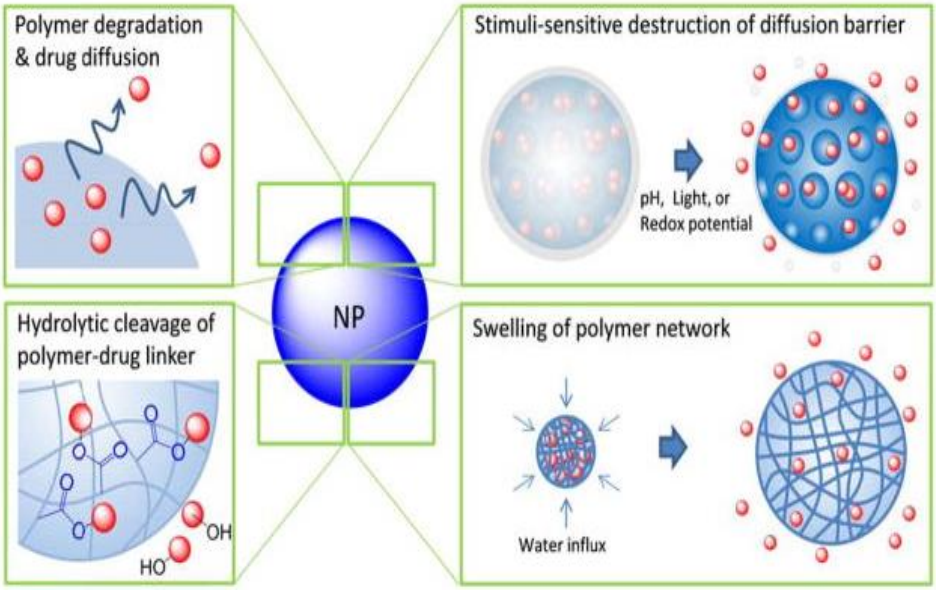

Figure 2.3 Drug release mechanisms employed in nanocarriers adopted from (Lee & Yeo, 2015).

2.5.1 Diffusion-controlled release

Diffusion-controlled drug release in which a drug is dissolved or dispersed in a core encircled with a polymeric membrane (Cauchetier, Deniau, Fessi, Astier, & Paul, 2003). Drug diffusion is driven by the difference in its concentration across the membrane (Crank, 2013). Where the drug dissolves in the core then diffuses via the membrane. matrix-type nano-sphere where drug molecules are dispersed throughout the polymer matrix also displays a diffusion-controlled release profile. In the matrix-type systems no membrane serves as a diffusion barrier; therefore, this system regularly shows high initial release followed by a decreasing release profile with the increasing diffusion of drug molecules located inside of the carrier.

2.5.2 Solvent-controlled release

Solvent transport into a drug carrier could influence the drug release pattern from the carrier. The solvent-controlled release incorporates osmosis-controlled release and swelling-controlled release (Langer & Peppas, 1983). Osmosis-controlled release appears in a carrier surrounded by a semi-permeable polymeric membrane via which water can pass from outside of the carrier with a low drug concentration to drug-loaded core with a high concentration of drug mechanism results in a zero-order profile as long as a constant concentration gradient is maintained via the membrane. . (Herrlich, Spieth, Messner, & Zengerle, 2012).

When hydrophilic polymeric matrices exist in an aqueous solution including physiological fluids, water diffuses into the system. The absorption of water results in the swelling followed by swelling-controlled release (Peppas, Bures, Leobandung, & Ichikawa, 2000).

The swelling-controlled systems include polymeric materials such as hydrogels whereas the mesh size presents a fundamental function in controlling the drug release behavior (Lin & Metters, 2006; Peppas et al., 2000).

2.5.3 Degradation-controlled release

Drug carriers that containing biodegradable polymers, such as polyamide, polyester, and polysaccharide, release the drug through enzymatic or degradation of bonds like ester, hydrazine or amide bonds in their original backbone (Lee, Mok, Lee, & Park, 2011; Prabaharan, Grailer, Pilla, Steeber, & Gong, 2009). The kinetics of the drug release are chosen and determined according to the existing polymer and the way the drug is released from it, which mainly depends on the functional groups, their number and their crystallization (Fredenberg, Wahlgren, Reslow, & Axelsson, 2011).

Biodegradable polymers are often preferred for their lysis to original components without causing side effects in the immediate and long range. The drug is released from its binding to the polymer by hydrolysis or enzymatically and here the links between the drug and the polymer carrying it are broken. The rate of the drug's dissociation from the polymer determines the drug kinetics of release. An enzymatic cleavage of bonds is usually used in what is called drug-targeting where the enzyme is clustered in certain places of the body (Medina et al., 2013).

2.5.4 Stimuli-controlled release

Stimuli-responsive release of drugs from its complex with polymers (nanocarrier) in response to an internal or external stimulus. These catalysts include temperature, pH, sound wave, magnetic or electric field, and ionic strength (Abouelmagd, Hyun, & Yeo, 2014). Since the release here is in response to a stimuli , we can use this method to drug-targeting (Song, Griffin, & Park, 2006). For example, the concentration of weak acidic drugs in the tissues of solid tumors (Min et al., 2010). These pH-sensitive carriers are similarly developed to determine a degree of drug release between extracellular and intracellular compartments (Talelli et al., 2010; Yuba, Harada, Sakanishi, Watarai, & Kono, 2013).

The drugs complexes could occur with thermo-sensitive polymers that transfer medications thermally and stimulated to release the drug (Chang et al., 2008; Li et al., 2011).

2.6) Studies on loading theophylline into other carriers

Salem and coworkers formulated theophylline nanoparticles using stearic acid either 5% or 10%. The resulting nanoparticles were stored at 4°C or frozen at −20°C, then lyophilized using a freeze dryer. The theophylline nanoparticles that were obtained had an average particle size of 290 nm and zeta potential of −39.5 mV, whereas the agglomerates were 2.47 μm in size with a zeta potential of −28.9 mV. The release profile was found to follow first-order kinetics ($r^2 > 0.96$). The nanoparticles and agglomerates resulted in a significant improvement in the release of theophylline (Salem, ME., Abo Eid, & Sharaf, 2011).

Was also investigated Microencapsulation of theophylline using different ratios of Eudragit S 100. The release profiles, the effect of stirring speed and different pH of dissolution medium on release profiles and stability were also studied. In vitro dissolution studies indicated that the rate of drug release was decreased with an increase in the amount of Eudragit S 100. The optimized formula was found to produce similar and sustainable release rate compared to the commercial product, Quibron T/SR tablet (Ahmad, 2012). Studied the release of theophylline from theophylline nanoparticles prepared with calcium alginate using an ionotropic gelation technique, honey was used as surfactant and stabilizer. The nanoparticles showed a remarkable swelling in the simulated intestinal fluid. The theoretical drug release values were validated with experimental values by considering diffusion and diffusion with swelling. It was found that after 3 h, the entire drug release followed a pure diffusion transport (Thomas, Nair, Latha, & Thomas, 2019). Theophylline Controlled drug delivery was prepared using polyvinyl alcohol (PVA) as a carrier with different molecular weight by electrospray method to optimize drug concentration in blood, decrease side effects, cause patient comfort and improve life quality.

Morphology and homogeneity of nanoparticles were investigated by scanning electron microscopy. The morphology of particles (10% concentration) was observed uniform and without fibers (Aminipour, Kolouei, Tohidi, & Bonakdar, 2018).

2.7) Theophylline-Chitosan Nanocomposites and Theophylline Loaded Nanoparticles

Chitosan has a great potential for forming polyelectrolyte complex (Yancheva et al., 2007). Ionic gelation method has been commonly used to prepare chitosan nanoparticles. In the ionic gelation method, the positively charged amino groups of chitosan interact with negatively charged polyanion to form nanoparticles. Tripolyphosphate is a polyanion that is commonly used to prepare chitosan nanoparticles by the ionic gelation method (Mohanraj & Chen, 2006).

In this method, the positively charged amino group of chitosan interacts with negatively charged tripolyphosphate to form coacervates with a size in the range of nanometer. Coacervates are formed as a result of electrostatic interaction between two aqueous phases, whereas, ionic gelation involves the material undergoing a transition from liquid to gel due to ionic interaction conditions at room temperature. So, in the liquid state and the acidic media, chitosan is characterized as its own group of ammoniums ($NH3^{+}$) that can combine with negatively charged tripolyphosphate. In **Figure 2.4**, we notice the interaction process of the ammonium group, of positively charged chitosan to form polyelectrolyte complexes.

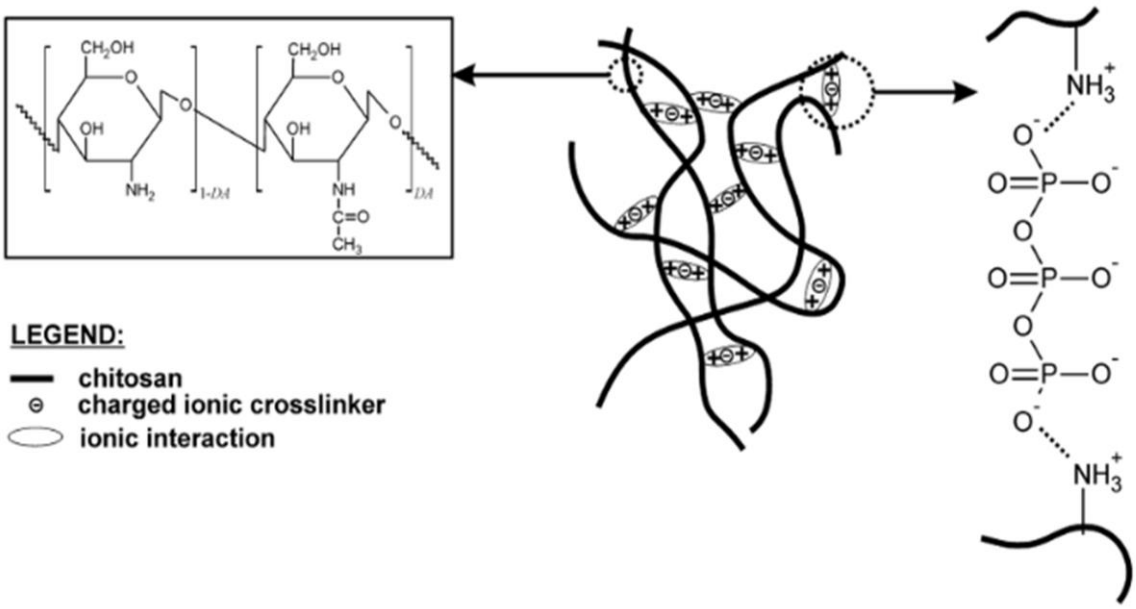

Figure 2.4 illustration of the ionic interaction in aqueous state between the ammonium group (NH_3^+) of chitosan and (PO_4^{-3}) of tripolyphosphate. (Pattanayek & Puranik, 2018).

CHAPTER THREE

METHODOLOGY

3.1) Chemicals

Theophylline (99%), and sodium tripolyphosphate (TPP) were purchased from Sigma Aldrich (pool,UK). Low molecular weight chitosan (10-120kD_a) from the Jordanian Pharmaceutical Manufacturing Company. Acetic acid and sodium hydroxide were bought from Chem Co (England), Water used was deionized.

3.2) Equipment

Table 3.1 Equipment used

Equipment	Company
Balance	**Sartorius, Germany**
Hot plate stirrer	**Labnet International**
Water bath sonicator	**BANDELIN, Germany**
Centrifuge	**Hettich Universal 30 RF, Germany**
Zetasizer	**Malvern Zetasizer Nano ZS (Malvern Instruments, Malvern, UK)**
UV-vis	**ShimadzuUV-1601 pectrophotometer**
Oven	**GALLENKAMP**
X-ray	**XRD-6000 diffractometer (Shimadzu, Tokyo, Japan)**
Infra-red	**Perkin Elmer (model Smart UAIR-two).**

Table 3.2 Levels of chitosan, TPP and pH

Parameter	Levels				
	1	2	3	4	5
chitosan in mg	50	75	100	150	*
TPP in mg	25	50	75	100	200
pH	4	5	6	6.5	*

3.3) Preparation of nanoparticle CSNPs

Chitosan nanoparticle were prepared by dissolving chitosan 500 mg in acetic acid 10 ml on 45 °C heat, stirring the sample to give formation of solution with uniform size, Then complete to 500 ml volumetric flask distilled water. 100 ml from this solution add to 500 ml volumetric flask then add tripolyphosphate dropwise on this solution to form chitosan nanoparticle.

3.4) Preparation of Theophylline loaded Chitosan Nanocomposites

Many researchers employed tripolyphosphate for chitosan nanoparticles preparation due to its valuable characteristics such as nontoxicity, multivalence and capability of making gels via ionic gelation because of its negative charge, theophylline-chitosan nanocomposites were prepared according to previously published research with some modifications (Panta & Negiab, 2018). Varied quantities of chitosan were dissolved in acetic acid under hot magnetic stirring (45°C).

As chitosan amount increased the amount needed of acetic acid increased to dissolve chitosan, tripolyphosphate was added dropwise to form CSNPs, then 100 mg of theophylline was liquefied in 15 ml of sodium hydroxide and completed to 25 ml using deionized water then added to chitosan nanoparticle to form THP-CSNPs. Monitoring pH value, when pH value low, raise it by using NaOH to achieve the specified pH (4, 5, 6 and 6.5). THP-CSNPs was subjected to stirring for 18 h. then centrifuged for 10_45 min depending on amount of chitosan was added to this sample, at speed of 11, 000 rpm, after completing the centrifugation a gel and a supernatant were obtained, dry the gel in oven on 40°C for two days to get dry powder of THP-CSNPs.

Table 3.3 Samples designed by full factorial designs

Run	Sample	Chitosan	TPP	pH
1	TCT 1	75	25	6
2	TCT 2	100	100	6
3	TCT 3	100	200	6
4	TCT 4	75	75	6.5
5	TCT 5	100	25	5
6	TCT 6	75	100	6
7	TCT 7	50	75	4
8	TCT 8	50	75	6.5
9	TCT 9	150	50	5
10	TCT 10	50	100	5
11	TCT 11	75	50	6.5
12	TCT 12	150	100	5
13	TCT 13	100	50	6
14	TCT 14	100	75	6.5
15	TCT 15	50	50	6.5
16	TCT 16	100	100	4
17	TCT 17	75	50	6
18	TCT 18	75	100	5
19	TCT 19	75	25	6.5
20	TCT 20	50	100	6.5
21	CT 21	50	200	4
22	TCT 22	100	25	6
23	TCT 23	50	50	4
24	TCT 24	75	25	5
25	TCT 25	75	100	4
26	TCT 26	150	75	5
27	TCT 27	100	100	5
28	TCT 28	150	25	6.5
29	TCT 29	50	50	6
30	TCT 30	100	75	4
31	TCT 31	50	25	6.5
32	TCT 32	50	50	5
33	TCT 33	150	50	4
34	TCT 34	150	25	6
35	TCT 35	75	75	4
36	TCT 36	50	200	6
37	TCT 37	150	25	4
38	TCT 38	75	50	4
39	TCT 39	100	50	6.5
40	TCT 40	150	50	6
41	TCT 41	75	200	5
42	TCT 42	75	50	5
43	TCT 43	100	75	5
44	TCT 44	150	100	5
45	TCT 45	150	100	6.5
46	TCT 46	100	200	4

47	TCT 47	100	100	6.5
48	TCT 48	150	75	6.5
49	TCT 49	150	25	5
50	TCT 50	100	50	4
51	TCT 51	50	75	5
52	TCT 52	150	200	6
53	TCT 53	150	100	6
54	TCT 54	75	200	6
55	TCT 55	100	200	5
56	TCT 56	100	75	4
57	TCT 57	100	25	4
58	TCT 58	150	200	6.5
59	TCT 59	150	75	6
60	TCT 60	100	25	6.5
61	TCT 61	150	75	4
62	TCT 62	150	200	5
63	TCT 63	100	50	5
64	TCT 64	75	25	4
65	TCT 65	150	50	6.5
66	TCT 66	150	100	4
67	TCT 67	75	75	5
68	TCT 68	75	75	6
69	TCT 69	50	25	5
70	TCT 70	50	100	6
71	TCT 71	50	25	4
72	TCT 72	75	100	6.5
73	TCT 73	100	75	6
74	TCT 74	50	200	6.5
75	TCT 75	50	25	6
76	TCT 76	75	200	6.5
77	TCT 77	50	75	5
78	TCT 78	50	100	4
79	TCT 79	50	75	6
80	TCT 80	50	200	5

3.5) Experimental

3.5.1 Ultraviolet Spectrophotometry

Ultraviolet-visible spectrophotometry is a popular technique extensively used for qualitative and quantitative characterization of samples. The measurement of absorbance was done at λmax=271 nm to measure the concentration of free drug (THP) in supernatant of sample solution after centrifugation, therefore, the percentage of

theophylline loaded (loading capacity) on the (chitosan) can be determined. Also, in vitro release of THP was determined in PBS (pH=7.4) by the same technique.

3.5.2 Fourier transform infrared spectroscopy (FTIR)

FTIR is used to identify functional groups and chemical bonds that exist in a molecule represented in the obtained spectrum of infrared absorption. Each functional group has its unique wavenumbers and absorption properties. Then, the functional group which exists in the sample can be deduced. Therefore, this technique can be used as supporting data, which may have encouraged the results of other techniques to indicate that interaction and compatibility. The spectra were obtained in the range of 400-4000 cm^{-1} on a Perkin Elmer with 4 cm^{-1} resolution. A small amount of powder sample was used (0.01mg) and force gauge was applied on the powder is about 75. Record and print the spectrum analysis from the instrument and clean the die with ethanol after finishing.

3.5.3 Particle size and zeta potential THP-CSNPs

THP-CSNPs particle size was measured by dynamic light scattering ((DLS): is a technique in physics that can be used to determine the size distribution profile of small particles in suspension or polymers in solution). With Zetasizer (Malvern, UK) at Hikma Pharmaceutical Manufacturing. Each sample was analyzed in triplicate at 25 C°. The samples were dispersed in distilled water then were sonicated for 15 minutes. The cuvette was filled and capped. Malvern logo should be directed to the instrument front and checking the absence of bubbles in the cuvette. The run numbers in each measurement was automatically defined by the software. The samples were prepared for zeta potential analysis as follows; disperse the sample in distilled water and measure zeta values at 25 ˚C. The procedure reported below:

a) Connect a syringe of 1 ml pre-loaded with the sample to a port of the cell.

b) Orient the cell upside-down (perts oriented down) and then slowly inject the sample reaching half of the loop formed at the bottom of the cell.

c) Checking that no bubbles are formed into the cell.

d) Return the cell in the vertical position (ports up).

e) Continue to inject the sample from the syringe.

f) Fill to the maximum level of the cell.

g) Then check that the electrodes are completely immersed in the liquid and there are no bubbles in the cell.

h) Remove the syringe and Cap the filled cells with its two caps.

i) Insert the cell into the instrument according to the instruction of the manufacture. Cells Malvern logo should be oriented towards the front of the instrument.

3.5.4 Theophylline loading efficiency

The ultra-centrifugation device was used to obtain the supernatant and measuring of the loading efficiency (LE) of theophylline from prepared nanocomposites. The steps were as follows:

1. The sample was centrifuged (Hettich Universal 30 RF, Germany) at 11,000 rpm for (10_45) min depending on amount of chitosan was added to this sample.

2. The free drug in supernatant was measured from the absorbance at λmax of 271 nm by UV-vis spectrophotometer.

3. The loading efficiency of theophylline was calculated from **the equation Eq (3.1).**

$$\%\text{Loading efficiency} = \frac{total\ amount\ of\ THP - total\ amount\ of\ free\ THP}{mass\ of\ nanoparticles}\ X\ 100 \quad \textbf{Eq (3.1).}$$

3.6) In Vitro Release Study of Theophylline from Nanocomposites

The release of dispersed theophylline was examined in PBS (pH 7.4), using a Perkin Elmer UV-vis spectrophotometer with λmax of 271 nm. A sufficient weight of each nanocomposite was added to 2 ml of the PBS. The cumulative amount of theophylline released into the solution was measured every 10 minutes by kinetic study in UV-vis spectrophotometer (whereas the device records the absorption reading every ten minutes as shown in appendix D) for 24 hours at corresponding λmax.

The percent of theophylline dissolving in the PBS was calculated from **Eq (3.2).**

$$\%\text{Release} = \frac{Concentration\ of\ THP\ at\ time\ t(ppm)}{concentration\ corresponding\ to\ 100\%release\ of\ THP(ppm)} X100$$

CHAPTER FOUR

RESULTS AND DISCUSSION

4.1) Optimization of variables and Selection of THP-CSNPs optimum formula

Among the different formulae of several compositions prepared, the choice of the optimum formula for theophylline loaded chitosan nanoparticles based on the ideal specifications that were determined using the Minitab 18 statistical program that is based on the analysis of the results. The integrative construction of the analysis relied on the three variables (Chitosan, TPP and pH) that are referred to as A, B and C respectively and at multiple levels for each variable.

The results represent what was obtained from the preparation of 80 samples of nanoparticles covering full factors combination and these results were statistically treated with using: i) Pareto chart, ii) contour plot,iii) surface plot,iv) interaction plot,v) main effects plot,vi) Normal probability plot,vii) versus order, viii) versus fits and ix) half normal plot.

All the factors displayed are separately modelled each as : (1) linear model, (2) Square model and (3) 2-way interaction model and these statistical parameters were conducted with the aim of knowing the effect of all variables on the size of the nanoparticles, the loading efficiency, and the zeta potential . Variables that were adopted by experiments and the results that were statistically processed after that include the effect degrees of chitosan, TPP, pH with their interaction effects. regression coefficients model was used and this is presented in **Table:(4.1)**. The reliability is considered of the linear, as well as square and also the 2-way interaction on parameters effectiveness when T-value and P-value less than 0.05.

Table (4.1) Results data for LE, zeta potential and particle size for Nanocomposites

Run Order	Sample code	Chitosan	TPP	pH	LE%	Particle size	Zeta potential
1	TCT 1	75	25	6	78	*	0.81
2	TCT 2	100	100	6	59	250	1.51
3	TCT 3	100	200	6	50	290	*
4	TCT 4	75	75	6.5	63	442	*
5	TCT 5	100	25	5	*	250	2.92
6	TCT 6	75	100	6	69	198	-7.37
7	TCT 7	50	75	4	*	250	1.53
8	TCT 8	50	75	6.5	*	300	-1.33
9	TCT 9	150	50	5	71	124	*
10	TCT 10	50	100	5	75	196	-7.39
11	TCT 11	75	50	6.5	68	250	3.54
12	TCT 12	150	100	5	*	*	*
13	TCT 13	100	50	6	*	*	-3.73
14	TCT 14	100	75	6.5	53	*	-1.02
15	TCT 15	50	50	6.5	78	290	-6.83
16	TCT 16	100	100	4	54	204	2.58
17	TCT 17	75	50	6	*	338	-3.83
18	TCT 18	75	100	5	63	*	-1.81
19	TCT 19	75	25	6.5	91	341	*
20	TCT 20	50	100	6.5	85	376	-4.44
21	CT 21	50	200	4	77	*	-0.34
22	TCT 22	100	25	6	*	309	*
23	TCT 23	50	50	4	79	*	13.91
24	TCT 24	75	25	5	*	146	11.11
25	TCT 25	75	100	4	71	*	-2.01
26	TCT 26	150	75	5	83	250	-0.12
27	TCT 27	100	100	5	66	298	0.62
28	TCT 28	150	25	6.5	91	296	-4.24
29	TCT 29	50	50	6	75	348	2.33
30	TCT 30	100	75	4	*	242	1.75
31	TCT 31	50	25	6.5	88	409	-1.08
32	TCT 32	50	50	5	70	180	7.44
33	TCT 33	150	50	4	86	312	1.85
34	TCT 34	150	25	6	92	225	-1.06
35	TCT 35	75	75	4	73	292	*
36	TCT 36	50	200	6	68	*	*
37	TCT 37	150	25	4	90	250	*
38	TCT 38	75	50	4	70	203	13.07
39	TCT 39	100	50	6.5	*	*	-3.44
40	TCT 40	150	50	6	84	250	-3.63
41	TCT 41	75	200	5	64	357	2.51
42	TCT 42	75	50	5	*	162	6.82
43	TCT 43	100	75	5	53	232	6.83
44	TCT 44	150	100	5	59	*	2.51
45	TCT 45	150	100	6.5	62	329	-2.06

46	TCT 46	100	200	4	*	391	-0.26
47	TCT 47	100	100	6.5	57	208	-0.08
48	TCT 48	150	75	6.5	66	250	-4.09
49	TCT 49	150	25	5	81	84	1.25
50	TCT 50	100	50	4	85	163	15.30
51	TCT 51	50	75	5	70	250	2.52
52	TCT 52	150	200	6	55	258	-2.12
53	TCT 53	150	100	6	75	250	-0.42
54	TCT 54	75	200	6	73	270	*
55	TCT 55	100	200	5	*	368	-7.62
56	TCT 56	100	75	4	50	309	-0.83
57	TCT 57	100	25	4	88	162	*
58	TCT 58	150	200	6.5	59	187	-0.95
59	TCT 59	150	75	6	62	*	-1.13
60	TCT 60	100	25	6.5	70	*	5.48
61	TCT 61	150	75	4	*	331	*
62	TCT 62	150	200	5	63	314	-4.44
63	TCT 63	100	50	5	67	119	*
64	TCT 64	75	25	4	91	110	7.08
65	TCT 65	150	50	6.5	86	268	-7.62
66	TCT 66	150	100	4	80	276	*
67	TCT 67	75	75	5	60	146	10.02
68	TCT 68	75	75	6	66	379	*
69	TCT 69	50	25	5	*	119	3.57
70	TCT 70	50	100	6	*	306	*
71	TCT 71	50	25	4	90	104	20.61
72	TCT 72	75	100	6.5	74	425	*
73	TCT 73	100	75	6	51	152	*
74	TCT 74	50	200	6.5	72	250	*
75	TCT 75	50	25	6	*	173	2.52
76	TCT 76	75	200	6.5	72	*	-9.12
77	TCT 77	50	75	5	83	*	1.17
78	TCT 78	50	100	4	83	250	1.53
79	TCT 79	50	75	6	*	284	-11.37
80	TCT 80	50	200	5	83	383	-10.26
***:** Deleted sample according to software suggestion.							

4.2) Impact of Formulation Factors on Loading efficiency, Zeta potential and Particle size

4.2.1 ANOVA outcomes for Loading efficiency, Zeta potential and Particle size

Regarding the results of the statistical studies (ANOVA) related to loading efficiency, they are shown in **Table (4.2) .**By using P-value (P-values) lower than 0.05 describe significant results. Through the results, and based on the value of P values using the models linear, square and third model (2-way interaction) found that (CS, TPP, pH, CS*CS, TPP*TPP, pH*pH and CS*TPP) are statistically significant. While, some variables were not significant such as (CS*pH and TPP*pH). To get better model (R^2 higher), the software deleted number of samples.

Table 4.2 ANOVA results for (loading efficiency)

Source	DF	Adj SS	Adj MS	F-Value	P-Value	VIF
Model	9	5966.87	662.99	12.88	0.000	
Linear	3	2835.46	945.15	18.36	0.000	1.31
CS	1	289.95	289.95	5.63	0.021	1.27
TPP	1	1532.53	1532.53	29.77	0.000	1.37
pH	1	461.41	461.41	8.96	0.004	1.09
Square	3	3030.73	1010.24	19.63	0.000	1.11
CS*CS	1	1272.96	1272.96	24.73	0.000	1.07
TPP*TPP	1	917.02	917.02	17.82	0.000	1.22
pH*pH	1	412.94	412.94	8.02	0.007	1.14
2-Way Interaction	3	629.37	209.79	4.08	0.011	1.37
CS*TPP	1	407.42	407.42	7.92	0.007	
CS*pH	1	47.46	47.46	0.92	0.341	
TPP*pH	1	78.42	78.42	1.52	0.223	
Error	52	2676.55	51.47			
Total	61	8643.42				

DF: Degree of freedom.
Adj SS: Adjusted sum of square.
Adj MS: Adjusted mean squares.
P-value: Lower than 0.05 significant result.
VIF: Variance inflation factor.

From **Table (4.2)** variance inflation factors (VIF) describe the multicollinearity. The VIFs has the advantage that it gives an idea of the increase in the variance of an estimated regression coefficient when the predictors used are correlated to each other. If all of the VIFs are 1, there is no multicollinearity, but if some VIFs are greater than 1, the predictors are correlated. When a VIF is > 5, the regression coefficient for that term is not estimated well. Also, the results appeared as shown in **table (4.2)** that, when using multi-factors, the model has low variance in the coefficient of regression, which means

a low in multicollinearity. Loading efficiency equations are mentioned and shown in **Table (4.3).**

Table 4.3 Regression equations for LE, PS and ZP in uncoded units

	Regression model
Equation 1	LE= 223.7 - 0.668 CS - 0.161 TPP - 41.6 pH + 0.004318 CS*CS + 0.001286 TPP*TPP + 4.11 pH*pH - 0.001140 CS*TPP - 0.0253 CS*pH - 0.0205 TPP*pH
Equation 2	Size= 455 + 3.20 CS + 5.25 TPP - 263 pH + 0.00040 CS*CS - 0.00105 TPP*TPP + 38.7 pH*pH - 0.00249 CS*TPP - 0.594 CS*pH - 0.769 TPP*pH
Equation 3	Potential= 59.6 - 0.014 CS - 0.2804 TPP - 13.07 pH - 0.001089 CS*CS + 0.000303 TPP*TPP + 0.493 pH*pH + 0.000675 CS*TPP + 0.0310 CS*pH + 0.0186 TPP*pH

R-square:

R^2: It is the percentage of the degree of variation in the response that belongs to each model. The goal of calculating R^2 is to know the suitability of the model used statistically with the results obtained from the completed experiments. The higher the value of R^2, this means that the model used is the best for expressing the analysis of the results of specific experiments. R^2 is always around (0-100) %. R^2 below 50% is indicating poor model.

R-sq. (adj.):

R^2 Adjusted is a modified form of the R Square, as it is adjusted according to the number of predictors in the model. R^2 Adjusted values are calculated based on the values of R^2as well as on the number of predictors and the sample size. Usually R^2adjusted is used when we want to compare a different number of predictors. The value of R^2 increases as we add an independent variable (predictor) if this predictor is ineffective and insignificant. On the other hand, we find that R^2Adjusted only when

predictor is significant and affects dependent variable. This helps in choosing the most correct and valuable model

R-sq. (pred.):

R^2 Predicted, it expects the predictive quality of the model you are using. Is calculation indicating that if you eliminate a data point from your data set, how much your model is capable to discover the correct value of that point, besides assessing the regression equation. Models that have higher predicted R^2 values, means better predictive conclusion. The value of R^2 predicted ranges (0-100) %. If the predicted R^2 is noticeably smaller than R^2, this is a sign of overfitting the model. In addition, it is certain that the expected R^2 may be more confirmed and useful than the adjusted R^2 in relation to model comparison because its calculation process takes place with observations that are not originally included in the calculation of the model.

Table 4.4 Regression model for dependent variables

	R-sq	**R-sq (adj)**	**R-sq (pred)**
LE	69.03%	63.67%	56.27%
Zeta potential	61.80%	55.06%	47.27%
Particle Size	57.32%	50.34%	40.64%

In terms of loading efficiency, the results are shown in **Table (4.4)**, and R^2 has been expressed as a measure of the ratio of total change that the model expresses. The value of R^2 was 69.03%. The value of R^2 was always increases by adding factors to the model even if these additions were insignificant and this explains the existence of expected problems with this statistic. (Kukreja, Chopra, Aggarwal, Khanna, & Optimization, 2011). On the other hand, the value of the adjusted- R^2 is computed as 63.67%, and the

calculated value of prediction- R^2 is calculated to be 56.27%. Statistically, this indicates that the loading efficiency model is shown around 56.27% of the new data variation and is in logical consistency with a value in adjusted- R^2.

Analysis of variance for the zeta potential is shown in **Table (4.5)** by means of P-value (P-values are lower than 0.05 describe significant results).

P- Values showed that the analysis models used (linear, square, and 2-way interaction) were significant for (TPP, pH and CS*CS). While some variables were not significant such as (CS, CS*pH, TPP*TPP, pH*pH and TPP*pH). When multiple factors are used in regression, this leads to the model being of low variance on coefficient of regression and thus considered small multicollinearity. In **Table (4.3)**, the accepted equation for calculating zeta potential values is mentioned.

Table 4.5 ANOVA results for zeta potential

Source	DF	Adj SS	Adj MS	F-Value	P-Value	VIF
Model	9	1409.85	156.650	9.17	0.000	
Linear	3	715.68	238.561	13.96	0.000	1.55
CS	1	2.46	2.462	0.14	0.706	1.08
TPP	1	429.21	429.214	25.12	0.000	1.49
pH	1	266.26	266.264	15.58	0.000	1.08
Square	3	143.48	47.826	2.80	0.049	1.04
CS*CS	1	83.93	83.932	4.91	0.031	1.05
TPP*TPP	1	50.59	50.590	2.96	0.091	1.50
pH*pH	1	6.28	6.281	0.37	0.547	1.33
2-Way Interaction	3	307.57	102.524	6.00	0.001	1.38
CS*TPP	1	108.29	108.287	6.34	0.015	
CS*pH	1	54.36	54.357	3.18	0.080	
TPP*pH	1	55.69	55.688	3.26	0.077	
Error	51	871.50	17.088			
Total	60	2281.35				

Regarding zeta potential results, From **Table (4.4)** the value of R^2 is 61.8%. The calculated value of adjusted- R^2 was 55.08%. Also, statistically, the value of predicted- R^2 was 47.27%. Because of the absence of the statistical difference between R^2 and adjusted- R^2 this showed a significant state that was involved into the model.

As for the particle size and the choice of the best form, a statistical model called full factorial design was used, which is a type of multi linear regression design. The three variables chitosan, TPP and pH and at multiple levels for each variable were the main factor in determining the best process, which gave us the best results. Eighty runs of nanoparticles production processes were performed and the Minitab-18 statistical software and several application programs plots were applied and this is shown in **Table (4.6),** which in general leads to expressing the role and impact of each of these variables on the size of the final nanoparticles produced. In **Table (4.6),** ANOVA of all these variables results is presented that signify the significant and non-significant variables that affect the particle size.

From **Table (4.6)** (Linear, square, 2- way interaction) (TPP, TPP*pH and CS*pH and pH*pH) had an important and direct significant effect on the size of the prepared nanoparticles because it had a value of P-value less than 0.05 and a higher value of F. However, it was found that the size of the nanoparticles did not significantly dependant on values of other variables such as non-significantly affecting on particle size at statistically significant level (P-value result above 0.05) such as (pH, CS, CS*CS, TPP*TPP and CS*TPP).

The results in this table had a clear confirmation of the results obtained from the Pareto chart of the standardized effects that was presented in Figure **(4.1)**.

Moreover, From **Table (4.4)** the value of R^2 is 57.32%. The calculated value of adjusted- R^2 was 50.34%. Also, statistically, the value of predicted- R^2 was 40.64%.

Because of the absence of the statistical difference between R^2 and adjusted- R^2 this showed a significant state that was involved into the model. The particle size equation is expressed in the multi linear regression mathematical model presented on in **Table 4.3.**

Table 4.6 ANOVA results for particle size

Source	DF	Adj SS	Adj MS	F-Value	P-Value	VIF
Model	9	261482	29053.6	8.21	0.000	
Linear	3	104191	34730.5	9.81	0.000	1.43
CS	1	867	867.0	0.24	0.623	1.14
TPP	1	98618	98618.3	27.86	0.000	1.47
pH	1	304	303.8	0.09	0.771	1.04
Square	3	42473	14157.7	4.00	0.012	1.04
CS*CS	1	13	12.6	0.00	0.953	1.05
TPP*TPP	1	663	663.4	0.19	0.667	1.34
pH*pH	1	40169	40168.9	11.35	0.001	1.09
2-Way Interaction	3	126510	42170.0	11.91	0.000	1.51
CS*TPP	1	1753	1753.5	0.50	0.485	
CS*pH	1	28239	28239.3	7.98	0.007	
TPP*pH	1	88485	88485.1	25.00	0.000	
Error	55	194689	3539.8			
Total	64	456171				

4.2.2 Pareto charts impact for LE, Zeta potential and Particle size

Pareto charts are used to identify the most statistically significant effect among multiple effects, depending on a curve graph and the arrangement of the effects from the largest to the smallest. In this chart, when you find columns that penetrate the curve, so these columns represent impacts that are statistically significant.

Regarding the loading efficiency, the effect of multiple variables on it, it was shown in the **figure (4.1.a)** .Pareto chart showed that the bars of (TPP, CS*CS and TPP*TPP) are

interaction with other variables (pH, pH*pH, CS*TPP, and CS) was passed through the reference line at the point (2.007). This indicates that these factors carry a statistically significant effect on the loading efficiency at P-level of (0.05). Also, this chart clearly shows that (TPP, CS*CS, TPP*TPP) had the highest significant effect on the loading efficiency compared to other variables. While, the loading efficiency was not statistically dependent (non-significant) on each of (TPP*pH and CS*pH).

Regarding the zeta potential, the results are presented in **Figure (4.1.b)**. Depending on the Pareto chart, it is clear that the main factors (TPP, pH, CS*TPP, CS*CS) cross the reference line in at (2.008). This means that these factors strongly influence the zeta potential values at the 0.05 level.

It also showed very clearly from the plot that TPP and pH had the greatest significant influence on the on-zeta potential than (CS*TPP) and (CS*CS) while (TPP*pH, CS*pH, TPP*TPP, pH*pH and CS) were not significant.

For the particle size aspect, From **Figure (4.1.c)**, the bars of (TPP, TPP*pH, pH*pH and CS*pH) are passed the reference line at (2.004). This means that these factors have an important and statistically significant effect on the particle size at the (0.05) level. From a more detailed aspect, and by relying on the Pareto chart, we find that it is quite clear that the (TPP and TPP*pH) have more effective and significant effect on the particle size than (pH*pH, CS*pH) and other variables. Whereas, particle size was not statistically significantly affected by either of (CS*TPP, CS, TPP*TPP, pH, CS*CS).

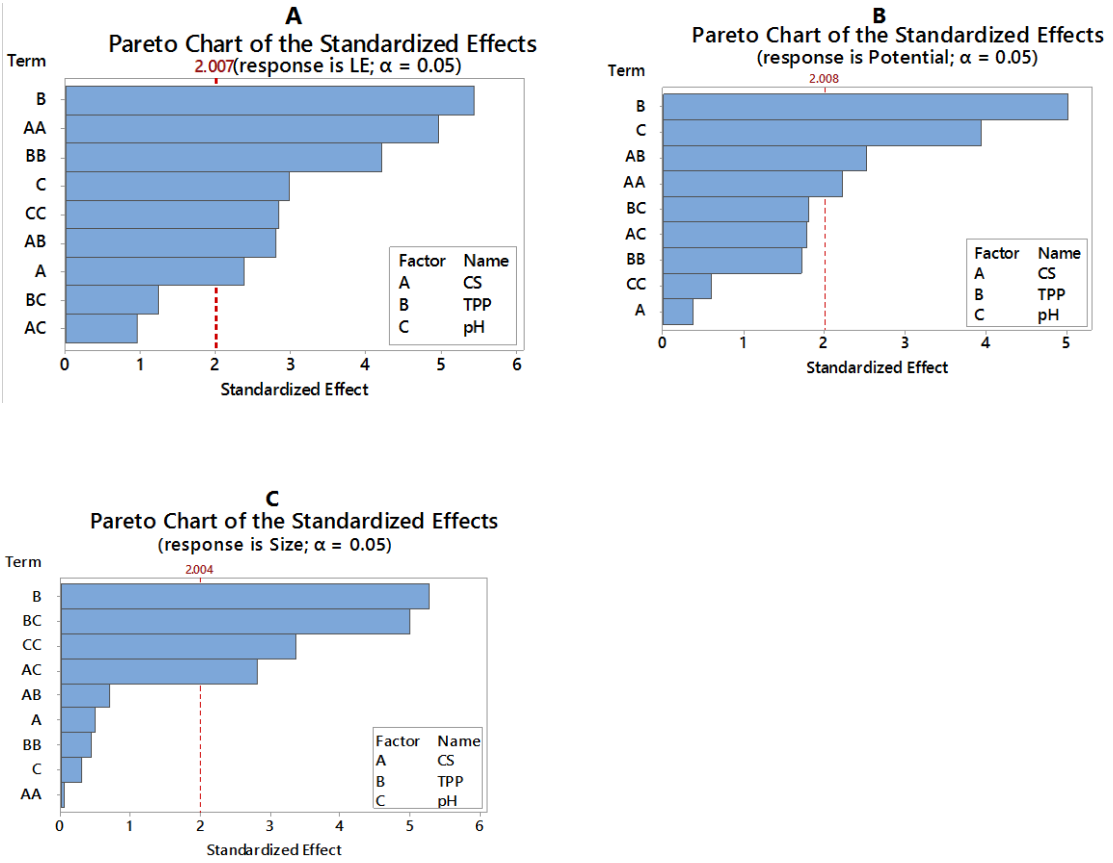

Figure (4.1) Pareto charts impact for (A) LE, (B) Zeta potential, (C) Particle size

4.2.3 Contour and surface plots impact for LE, zeta potential and particle size

The purpose of using Contour Plot in this study is to identify the potential relationship between the three variables, namely (Chitosan, TPP, and pH).

Contour Plot has the advantage that it displayed a two-dimensional relationship with X and Y factors (i.e. predictors) plotted on the scale X and scale Y, and here we see a response values appear in the contours. With respect to surface plot, like a topographical map wherein x, y, and z values are designed and plotted in preference to longitude, elevation and latitude. Three dimensions (3D) surface plot is graph can be used to identify the potential relationship between three variables. Predictor variables are presented on the x and y scales, and here the response variable (z) appears as a smooth

surface (3D diagram). The loading efficiency response is shown in the illustrations in **Figure 4.2.** From **Figure (4.2.(C-1))** that there are two regions of highest loading efficiency (more than 80%) when pH is 6 to 6.5 or less than 4.6 and the amount of TPP is less than 50 mg, This reinforces the information mentioned previously in the **Table 4.2** as both TPP and pH were statistically significantly affecting on loading efficiency.

On the other hand, the Contour plot response, which analyzes the pH and chitosan relationship in loading efficiency, is presented in **Figure (4.2. (B-1))**.

Therefore, when the chitosan used in small amount (about 50 mg) or ≥130 mg with a pH in between 6 and 6.5 or less than 4.25 the loading efficiency is being larger than 70%. When the TPP used in small amount (less than 50 mg) and chitosan less than 50 mg or ≥130 mg, this results with a loading efficiency being larger than 80%.

It is useful that surface plots can give a three-dimensional curvature that clearly shows the process of change in the loading efficiency according to the different factors affecting this; of course, it is useful in the process of combining the output values and the various variables. In these graphs, the variables are displayed on the X and Y axes, while the outputs are displayed on the Z axis. As the surface becomes darker, this means an increment the response. Therefore, high loading efficiency can be achieved by using amounts of chitosan that are approximately 50 mg, pH around 6 and using TPP less than 50 mg.

The loading efficiency was higher at upper and lower levels of pH than at middle pH, this may be attributed to high charge density of chitosan and TPP at low and high pH.

At low amount of TPP .i.e. high chitosan/TPP ratio , the chance of interaction between chitosan and theophylline are higher since the number of positive charges versus that of negative charges has increased, and a higher loading efficiency is expected (Karimi et al., 2013).

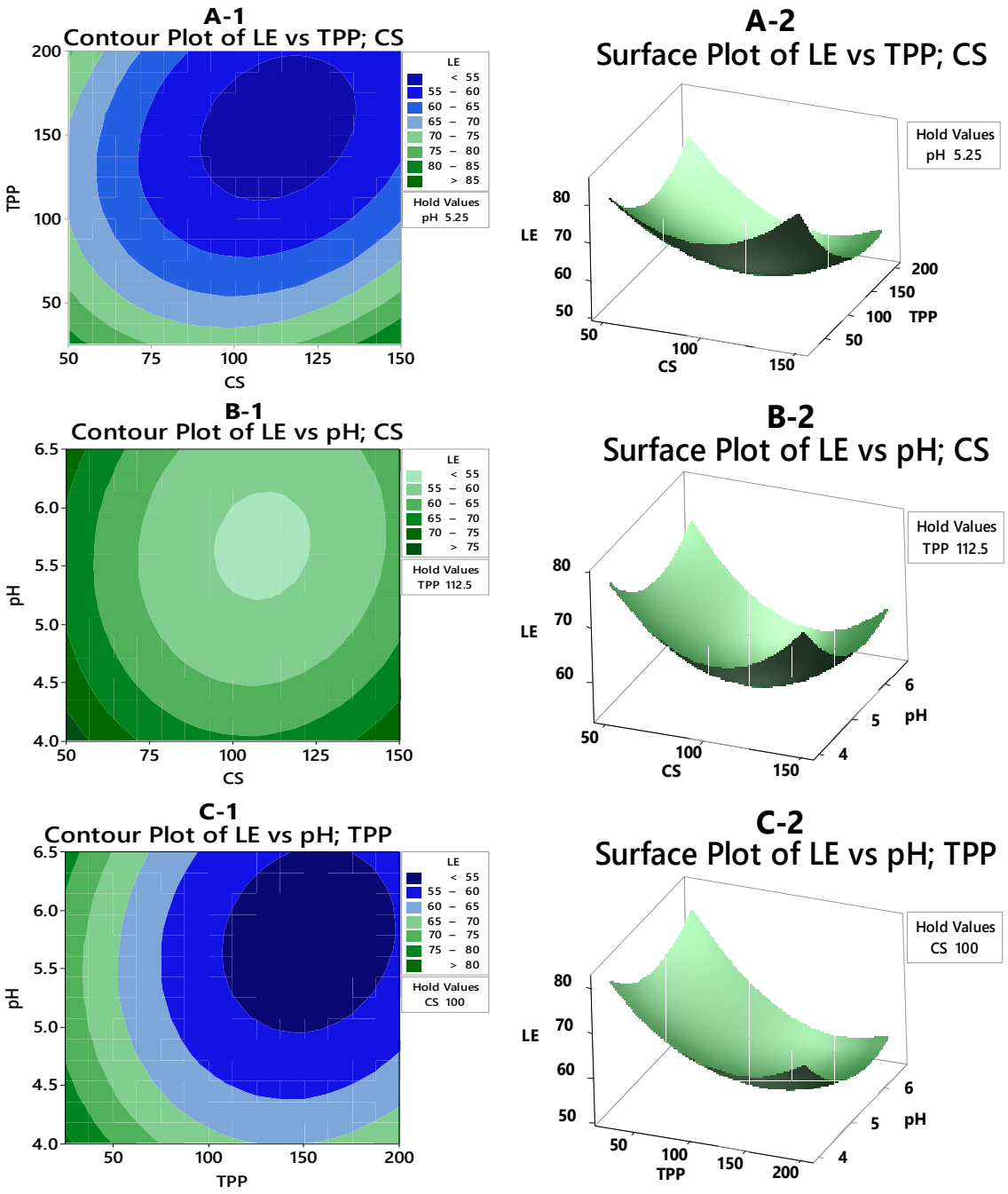

Figure (4.2) Contour plots and surface plots for LE against pH, TPP and chitosan variables

It is clear from **Figure (4.3. (C-1))** that the highest zeta potential region was when pH is less than 5 and the amount of TPP is ≤ 60 mg but the % of zeta potential is between (8-12 mV), This gives support to the previously mentioned information **in Table 4.3** as both TPP and pH were expressively affecting the value of zeta potential. In addition, the response of the Contour plots to the effect of the pH and the amount of chitosan on the value of zeta potential were presented in the **Figure (4.3.(B-1))** . When the amount of chitosan used between (50 mg to 125 mg) and, pH is less than 4.5, zeta potential is getting larger than 2mV but it still low, this gives support to the previously mentioned information in **Table 4.3** as CS was not significantly affecting zeta potential. **Figure (4.3.(A-1))** showed that when TPP less than 50 mg and CS is between 50 and 125, zeta potential was more than 5 mV which is still low. From surface plots, then, highest zeta potential can be achieved by using pH is < 5 and using amount of TPP ≤ 50.

The zeta potential decreased due to the neutralization of protonated amino groups by TPP anions (Zhiyang et al., 2020).

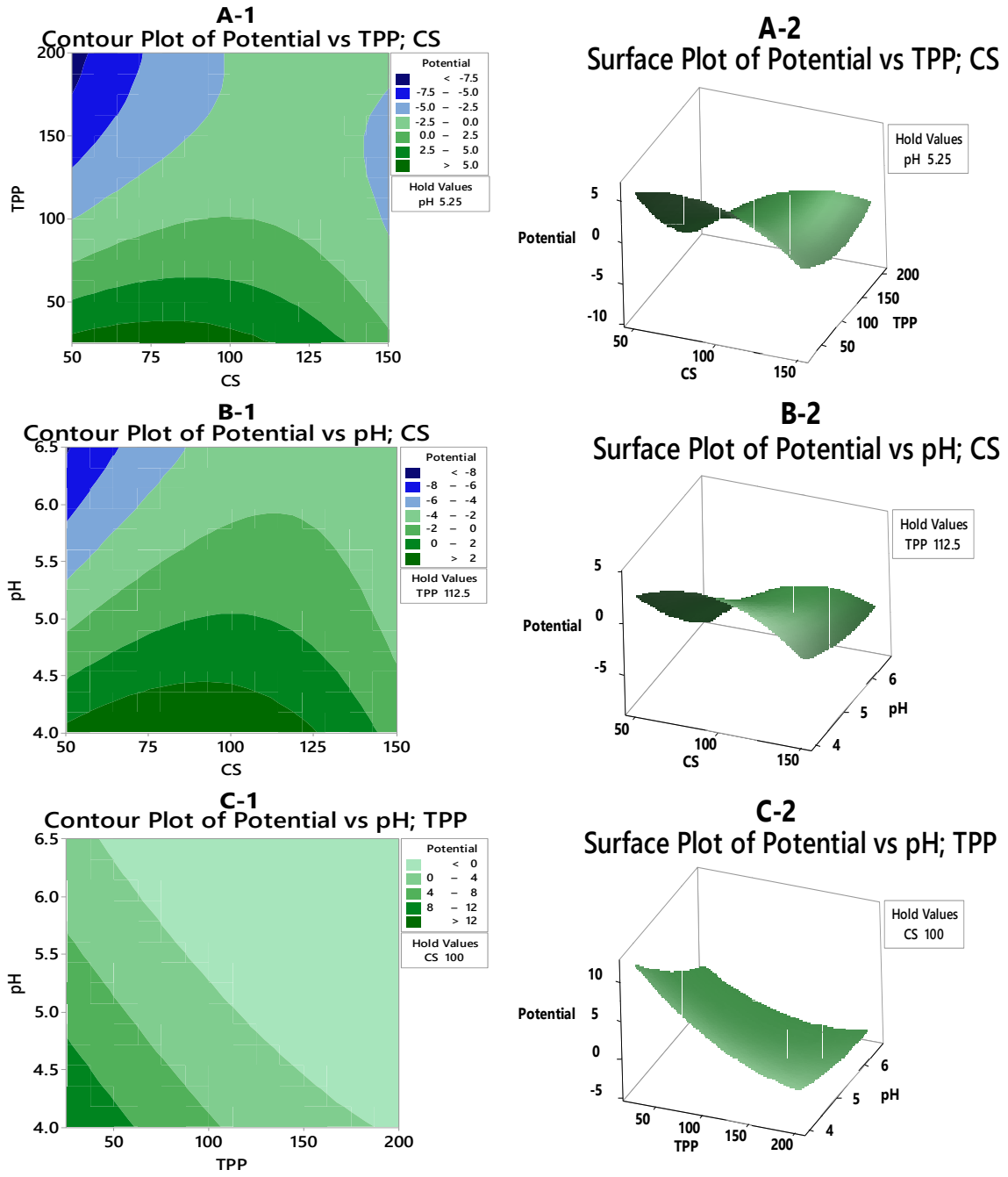

Figure (4.3) Contour plots and surface plots for Zeta potentioal against pH, TPP and chitosan variables

It is apparent from **Figure (4.4.(C-1))** that the size of the particles still less than 150 when the amount of TPP is less than50 mg and pH less than 5.5, This gives support to the previously mentioned information in **Table (4.4**) as TPP was significantly affecting the particle size. Furthermore, the response contour plots to the analysis of the power of pH and amount of chitosan on the particle size were illustrated in **Figures (4.4. (B-1) and (B-2))**. When chitosan is used in an amount more than 125 mg and, pH is more than 5, the particle size is getting less than 200 nm. **Figure (4.4.(A-1))** when TPP ≤150 mg, the particle size was lesser than 200 nm and no effect of chitosan as previously was mentioned in **table 4.5.** Surface plots as showed in figure **(4.4(C-2)**) the size of particles was less than 50 nm when TPP was less than 50 mg and pH was less than 5.5.

If the amount of TPP is high this lead to aggregation or formation of nanoparticles with larger particle sizes (Vyas et al., 2010).

Particle size may vary with pH as a result of a change in zeta potential (or effective net charge) of the particles .Therefore, as the pH increased many nanoparticles may aggregate.

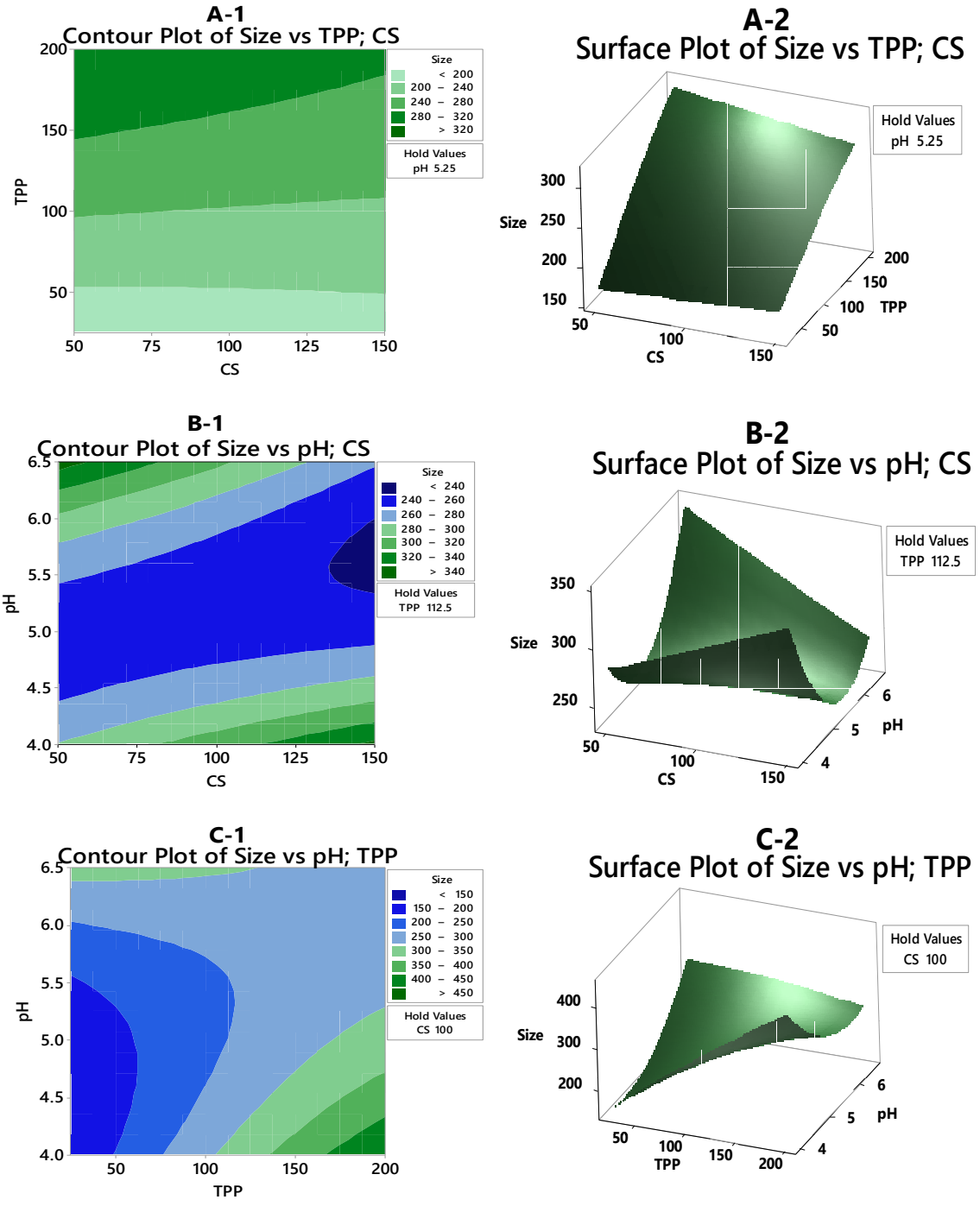

Figure (4.4) Contour plots and surface plots for Particle size against pH, TPP and chitosan variables

4.2.4 Main effect plots for LE, zeta potential and particle size

The aim of using a main effects plot is to identify the significance of each variable on different levels, there are effects related to the role of different levels and concentrations of a given factor in producing different responses. The main effect plots curve represents the response mean for any variable that are associated with a line.

Regarding loading efficiency,

Figure (4.5.a) shows the main effect plot, from which we conclude that (chitosan, TPP and pH) are factors that have a definite effect on the loading efficiency, and that, with increasing the concentration of chitosan, the loading efficiency has begun to decrease until the amount of chitosan reaches 100 mg. Then we find that the increase in the amount of chitosan is more than 120 mg then the LE was increased. While when concentration of TPP was increased, the LE lean towards a decrease till the concentration of TPP reached 150 mg. When TPP concentration was increased more than about 150 mg the loading efficiency was increased. Finally, by increasing pH, the LE lean towards a decrease until about 5.75 then when pH is elevated more than 6 the LE was increased**.**

Regarding zeta potential

From **Figure (4.5.b)** offered the results by using the main effects plot, which Indicated that (chitosan, TPP and pH) were factors that have a definite effect on the zeta potential. By elevating the concentration of chitosan, the zeta potential tended to slightly increased until the amount of chitosan reached 100 mg. When chitosan amount increased more than about 120 mg the zeta potential was decreased. While, by increasing TPP concentration, the zeta potential tended to be decreased till the amount of TPP reached 200 mg. Also, by increasing pH, zeta potential tended to decreased until 6.5.

Regarding particle size

From **Figure (4.5.c)** offered the results of main effects plot, that displayed that chitosan was factor that had almost no effect on particle size. While, by elevating TPP concentration, the particle size lean towards to increase. The size decreased when pH increased till 5.5 then tended to increase.

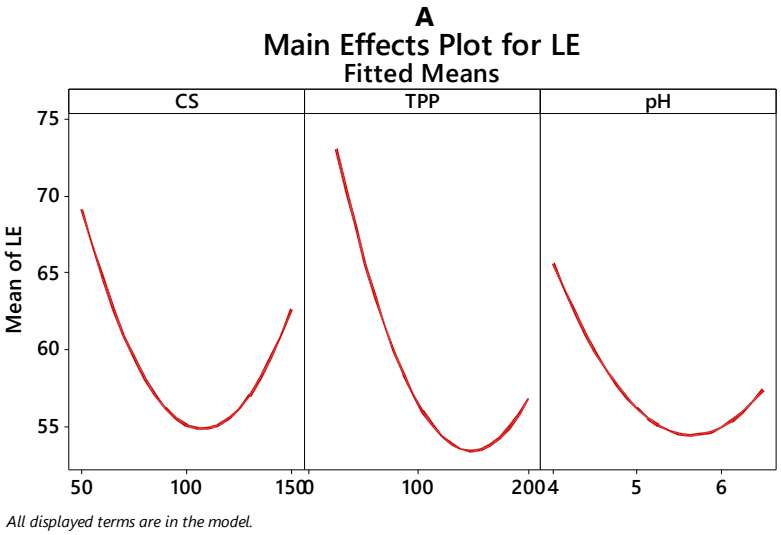

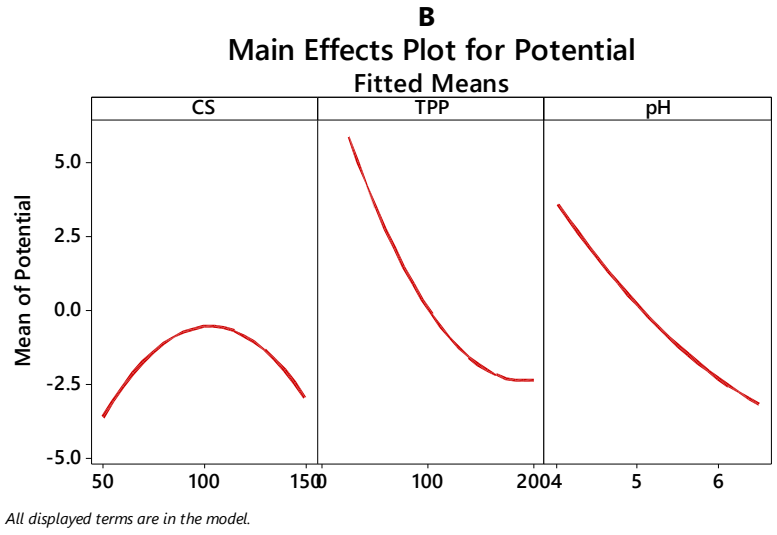

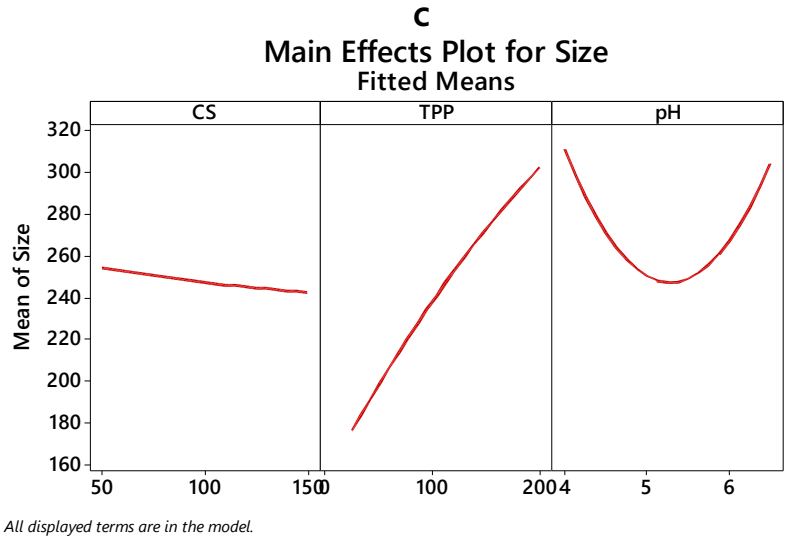

Figure (4.5) Main effect plots for LE, zeta potential and particle size

4.2.5 Interaction plots for LE, Zeta potential and Particle size

Interaction plot is used to follow any possible interactions in which the influence of any factor depends in one way or another on the level of another influencing factor. This plot contains the setting of different levels of one influencing factor in the x-axis with the presence of another line for another factor and at different levels. When there are parallel lines then that it means that there is no interaction between the factors. The higher the degree of variation in the slope between the two lines, the higher the degree of interaction

Regarding loading efficiency

Figure (4.6.a) shows the interaction between loading efficiency with regards to chitosan depending on the different values of TPP and pH. Since the results showed that the lines are not parallel, and this means that there is an interaction that is significant between loading efficiency and chitosan depending on different levels of TPP and pH.

Regarding zeta potential, figure (4.6.b) the effect shows the interaction between zeta potential with regards to chitosan dependent on different values of TPP and pH. Also, since the results showed that the lines are not parallel, and this means that there is an interaction that is significant between zeta potential and chitosan depending on different levels of TPP and pH.

Regarding particle size, **figure (4.6.c)** shows the interaction between particle size with regard to chitosan depending on the different values of pH because the lines are not parallel, that indicates an interaction that is significant between the chitosan and particle size depending on different levels of pH. But no significant interaction was noted between chitosan and particle size at different levels of TPP.

A

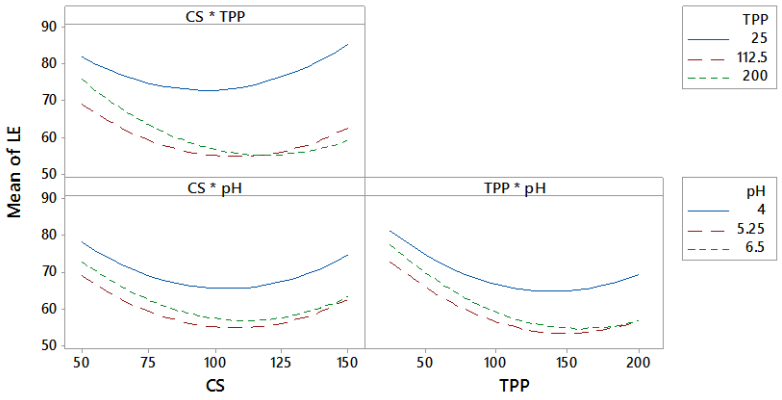

All displayed terms are in the model.

B

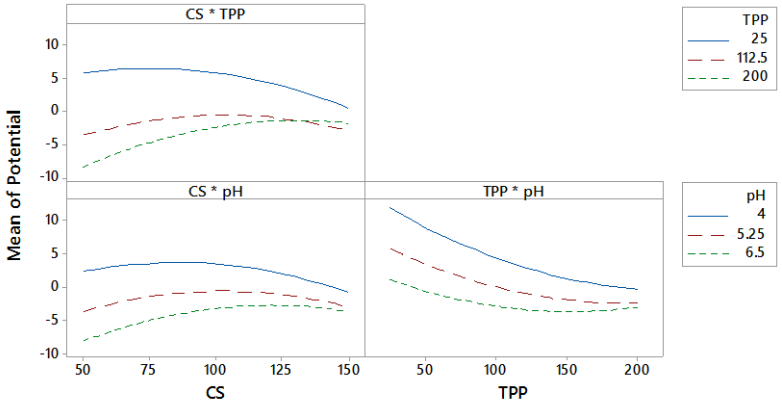

All displayed terms are in the model.

C

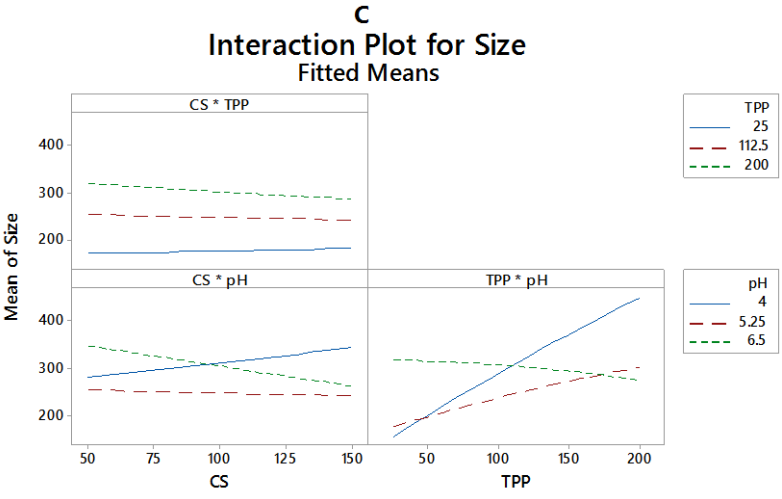

All displayed terms are in the model.

Figure (4.6) interaction plots for LE, zeta potential and particle size

4.2.6 Residual plots for LE, zeta potential and particle size

A residual plot is a curve graphic used to illustrate the quality of fitting goodness in regression and ANOVA. The purpose of using normal probability plot is to demonstrate the model in which the residuals in the normal condition are distributed. Through the data provided in **Figure (4.7)**, a nearly straight line for the normal probability plot can support the model chosen to study the effect of multiple variables on loading efficiency, zeta potential, and particle size.

Figure (4.8) explains the residuals versus the order plot and **Figure (4.9)** explains the residuals versus the fits plot for the loading efficiency, zeta potential and particle size. The use of the residuals versus order plot to confirm the model that the residuals do not depend on each other. Ideally, on the plot, the residuals should randomly fall around the center line. While, versus fits plot, the use of the residuals was to confirm the model that the residuals are distributed randomly, and it has a constant variance. Ideally, points must fall randomly on both sides. In general, these results showed that the plots do not follow a systematic approach. Therefore, this model does not have any possibility of systematic errors.

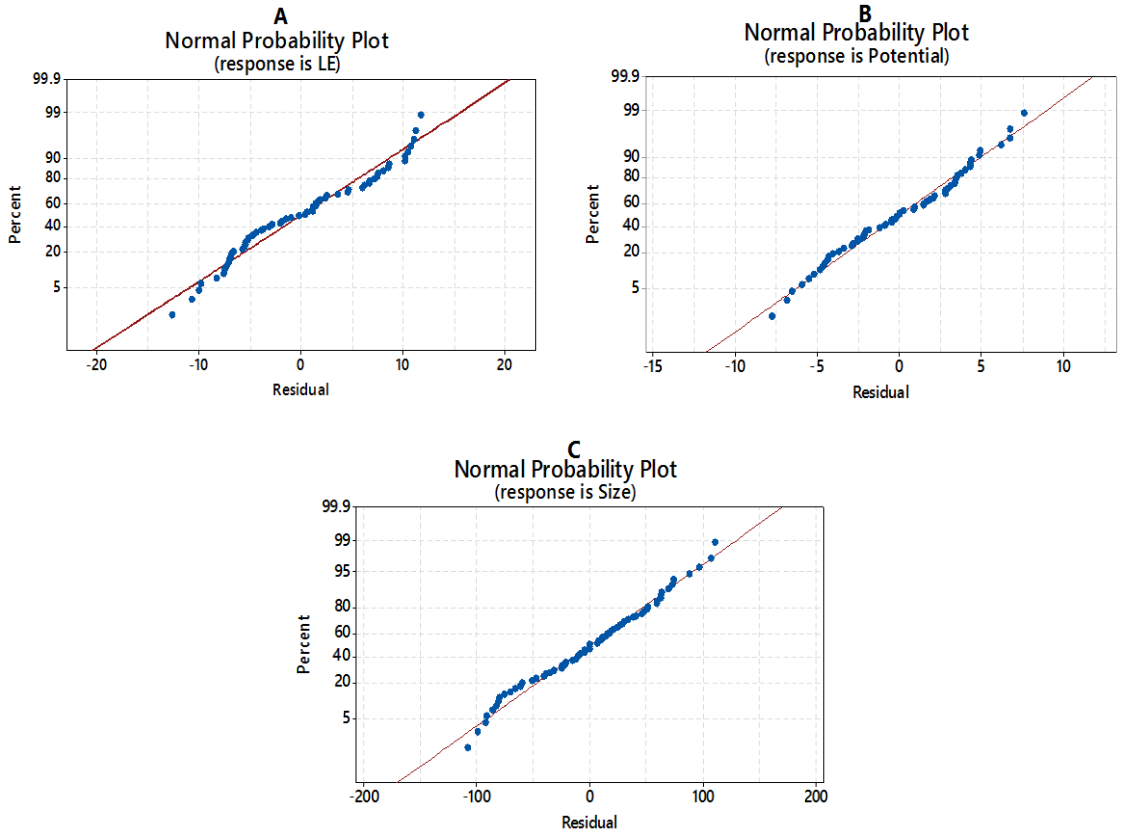

Figure (4.7) Normal probability plots, LE, ZP and PS of residuals

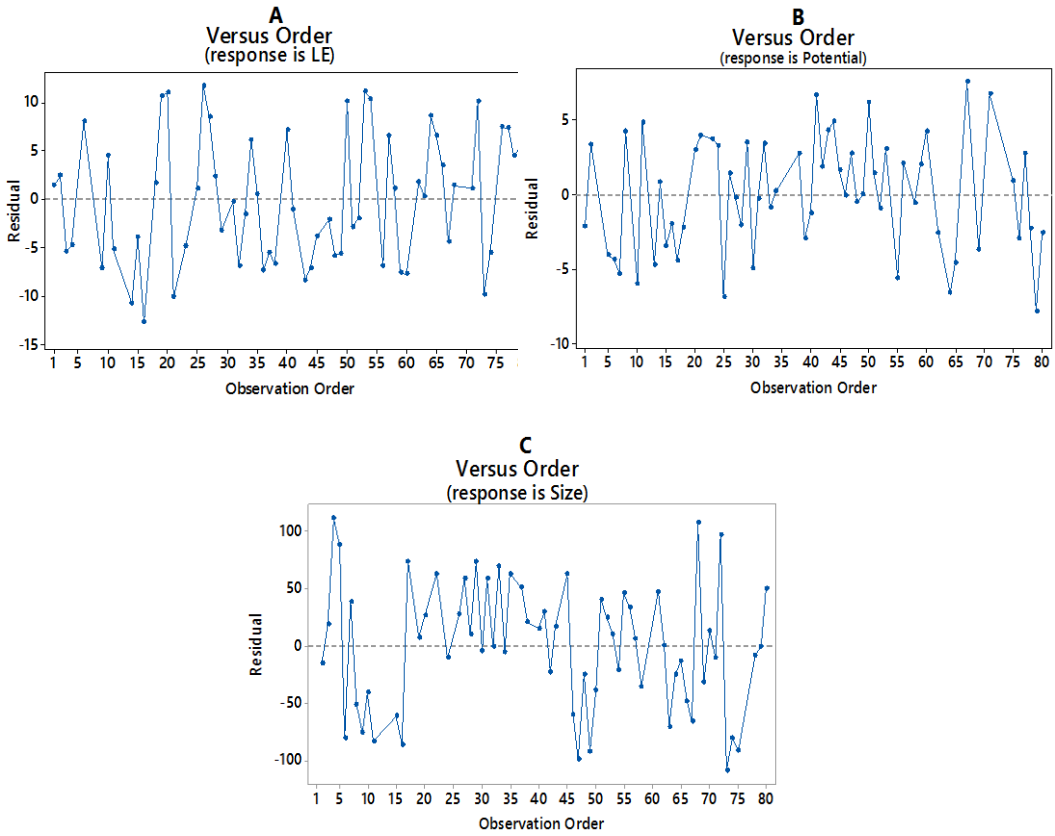

Figure (4.8) Residual versus order of data for LE, ZP and PS

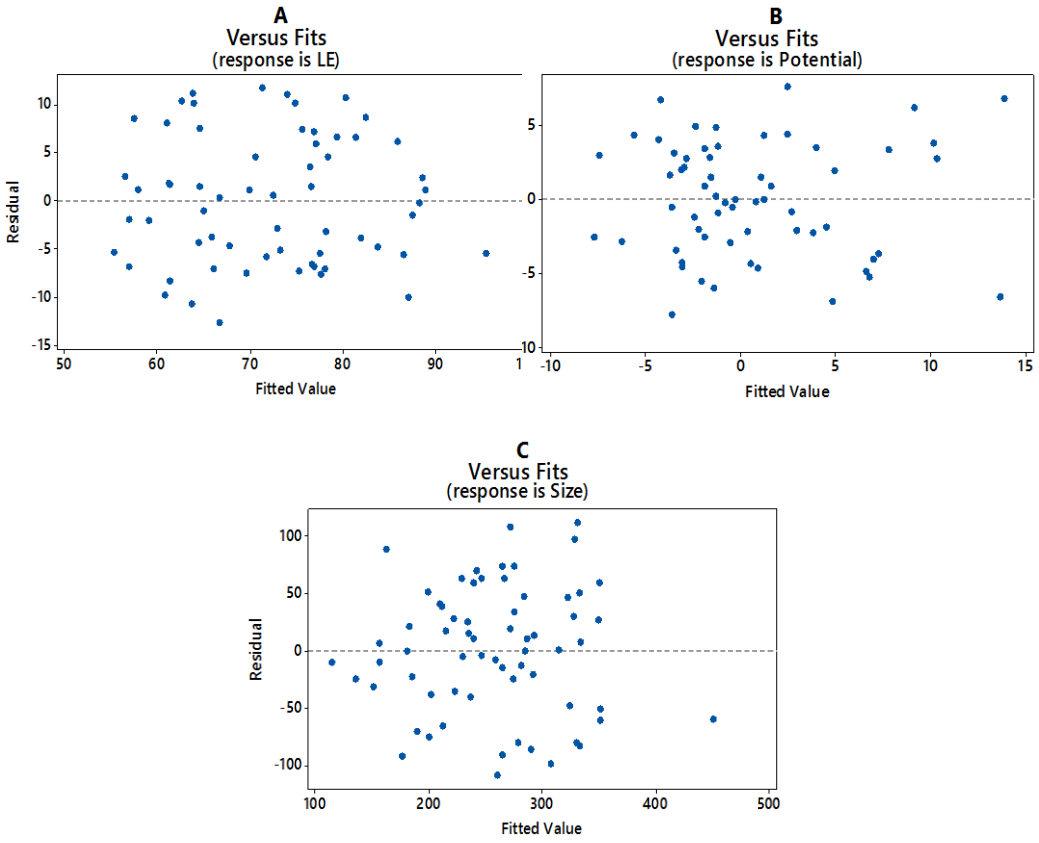

Figure (4.9) Residuals versus fits of data for LE, ZP and PS

4.2.7 Half normal plot effect

The aim of using the half normal probability plot is to identify and determine the magnitude and importance of any effects. In the half normal probability plot of the effects it is indicated that the effects that are further than zero are significant statistically. In these plots, the shape and color of the points are different between statistically significant and nonsignificant effects. Parameters are labeled significant on the graph when the P-value below 0.05. From **Figure 4.10** concluded that the TPP and chitosan have a significant effect on LE, zeta potential and particle size. And TPP is higher than chitosan in that aspect. On the other hand, pH has no significant effect on the response significantly except on zeta potential.

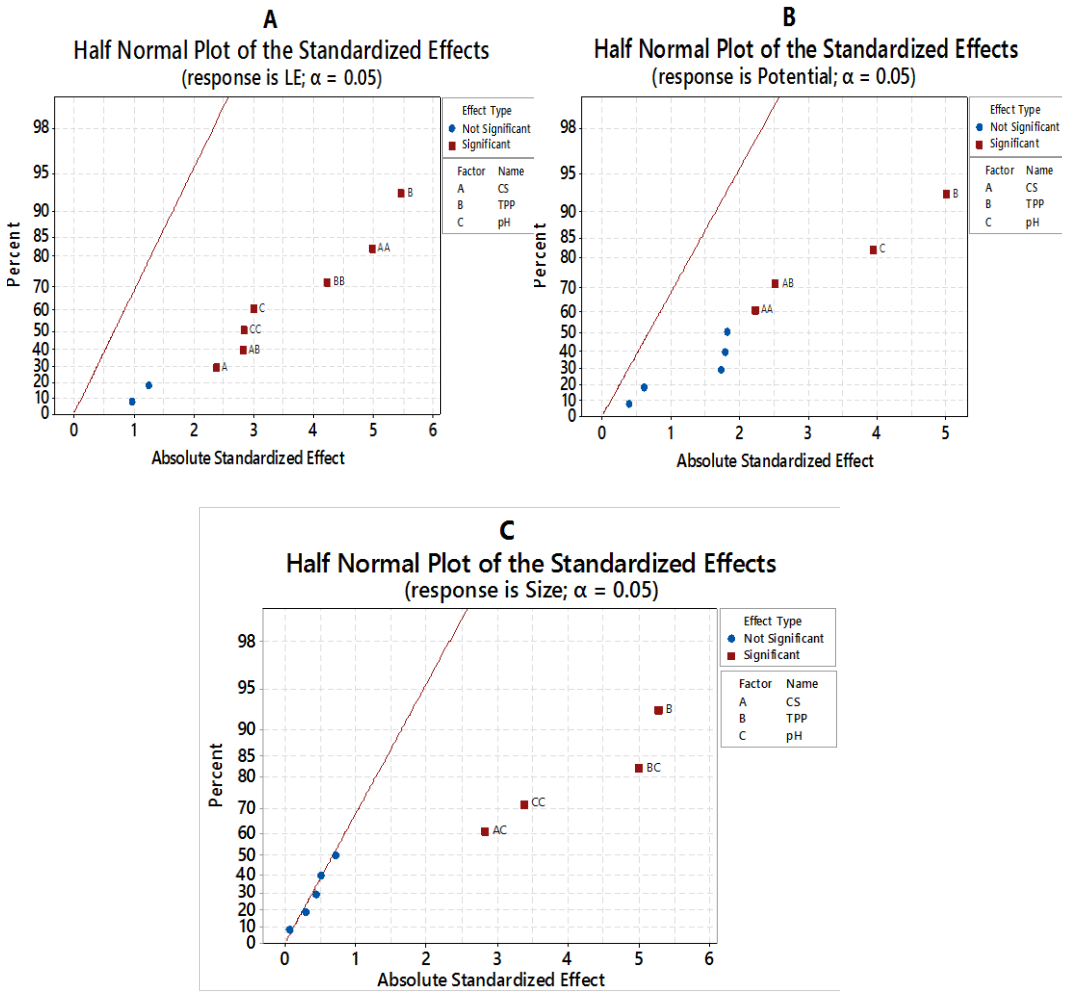

Figure (4.10) half normal plot for (A) LE, (B) zeta potential and (C) particle size

4.3) Optimization and validation of three models

Table 4.7 Comparative results between observed and predicted response values of variables of optimized formulation

concentrations	Experimental response	Predicted values	Experimental values	Bias (%)
CS (50 mg) TPP (25 mg) pH (4.3)	LE (%)	88.8%	80.1%	9.8%
	Particles size (nm)	342 nm	405 nm	-18.4%
	Zeta potential mV	13.9 mV	11.1 mV	20.1%
CS (109 mg) TPP (104 mg) pH (5.3)	LE (%)	55.6%	62.3%	12.1%
	Particles size (nm)	241 nm	200 nm	17.0%
	Zeta potential mV	-0.5 mV	-15.0 mV	17.2%
CS (134 mg) TPP (157 mg) pH (4.6)	LE (%)	59.4%	52.0%	12.5%
	Particles size (nm)	321 nm	347 nm	8.1%
	Zeta potential mV	1.3 mV	11.0 mV	8.3%

Note: the Bias was Calculated by following equation (predicted value - experimental value/predicted value) ×100%.

To compare the experimental values with the predicted values, a bias formula was performed underneath optimized factors.

As exposed in **table 4.7**, the amount of bias was about 9.8%, -18.4% and 20.1% for the first formula (CS=50 mg), (TPP= 25 mg) and (pH 4.3). While, the bias was about -12.1%, 17% and -17.2% for second formula (CS=109 mg, TPP=104 mg, and pH=5.3), the values of bias were 12.5%, -8.1% and 8.3% for the third formula (CS=134 mg, TPP=157 mg, and pH=4.6). These results and data through which we conclude the validity and effectiveness of the generated models with statistically non-significant differences in addition to good correlation between the experimental and the predicted values.

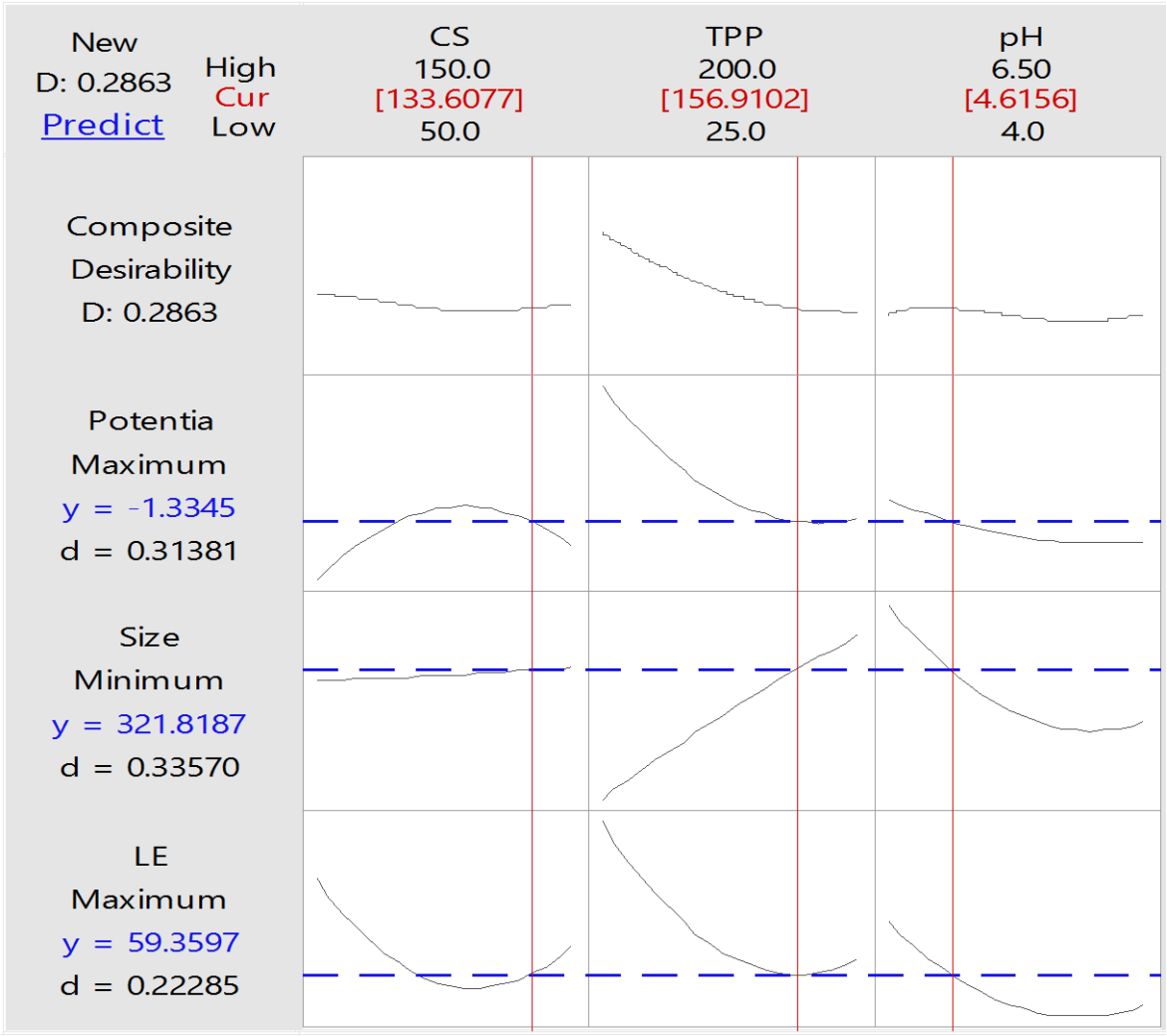

Figure 4.11 Optimized concentration for response factors of LE, ZP and PS.

Through the previous figure. When moving the red line, new default values for each of chitosan, TPP and pH can be obtained. Therefore, changing the values of the previous three variables will give new predicted values for LE%, zeta potential and particle size. In the laboratory, the experimental values for LE%, zeta potential and particle size were obtained. Calculate the difference between the experimental values and the predicted values by using the Bias equation.

4.4) Fourier transform infrared (FT-IR)

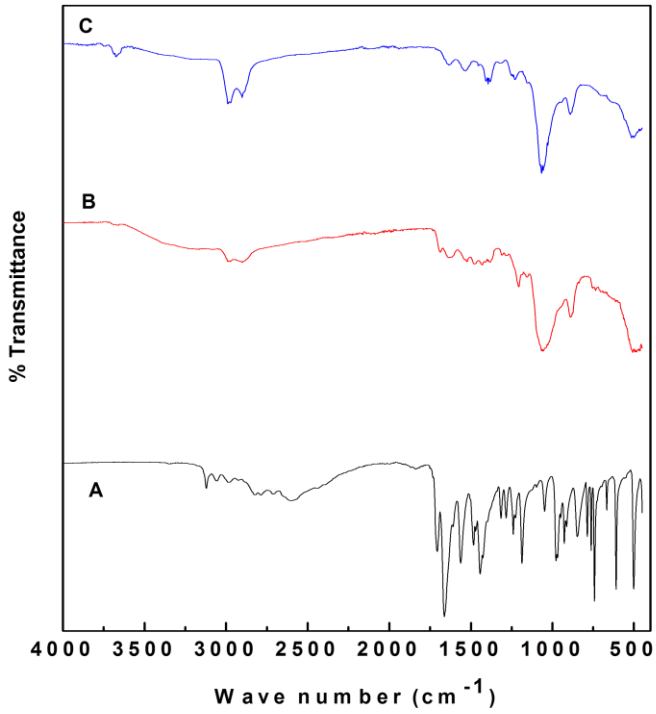

Figure 4.12 Infra-red spectra of THP (A), CS nanoparticles (B) And THP-CSNPs (C)

Figure 4.12 appears FTIR spectra of THP, CS and THP-CS nanocomposite respectively. FTIR spectra **(Fig. 4.12. A)** Showed that the Theophylline has distinct peak values at 1718 cm^{-1} and 1665 cm^{-1} which they are related to the asymmetric and symmetric stretching vibrations, respectively. These two peaks accounts to the two groups of carbonyl groups (C=O). We also note from the drawing that there is a peak at 1567 cm^{-1}, allocated to the C=N stretching vibrations. (Fini, Cavallari, Ospitali, & Gonzalez-Rodriguez, 2011). For CS nanoparticle **(Fig. 4.12. B)**, an absorption peak was 3200 cm^{-1} due to OH and

NH2 stretching. A peak at 2868 cm^{-1} assigned for CH stretching. Absorption bands at (2800–2900) cm^{-1} , 1650 cm^{-1},and 1574 cm^{-1}, are due to C–N stretching ,amide band, and N–H bending, respectively. (Tığlı Aydın & Pulat, 2012).

Asymmetric stretching peak of C–O–C is evident around 1151 cm^{-1}. Two peaks for amine and N–H bending vibration present that shifted to 1534 cm^{-1} and 1432 cm^{-1}, respectively, and this can be explained by the strong ion cross linking and interference of chitosan with TPP. (Tığlı Aydın & Pulat, 2012). Another peak at 1156 $cm^{-1}$was present and its due to C–O–C and P=O. (Nallamuthu, Devi, & Khanum, 2015). The mentioned results can be ascribed the linkage between the ammonium group of chitosan and the phosphoric group of TPP in nanoparticles. The THP-CSNPS sample showed the same characteristic peaks with fewer shifting.

4.5) In vitro release study

Release profile curves of theophylline from the nanocomposites (THP-CSNPs) are presented in **Figure (4.13).** The release testing at pH 7.4 reporting the amount released versus time. It can be observed that the released theophylline from nanoparticles in the samples (TCT1, TCT 66 and TCT 54) after 8 hours reaapproximately reached 30, 48, 25%, respectively. Whereas the amount released from nanoparticles in sample (TCT62) reached 60% after 10 hours. The process of releasing theophylline from nanocomposites can be organized and explained by several mechanisms. The first method is the hydrogel swelling process by taking water in the release medium through the polymer and the resulting swelling and solubility that leads to the release of the drug. (Mahdavinia, Mosallanezhad, Soleymani, & Sabzi, 2017). The second explanation is the diffusion and erosion of the polymer, and then the drug is

released. This usually happens from the matrix containing chitosan. In the diffusion the drug permeates and penetrates through the polymer matrix to the surrounding areas. In the case of erosion, the polymer is crushed and degraded, thus the bonds are broken and the drug is released. The third explanation for the drug release process is through disintegration, which is dependent on many factors, such as the enzymes present in the dissolution medium, pH of the medium and its effect on the polymer's activity. Also, interfering of samples with other polymers and taking water by these polymers thus freeing the drug (Fonseca-Santos, Satake, Calixto, Dos Santos, & Chorilli, 2017).

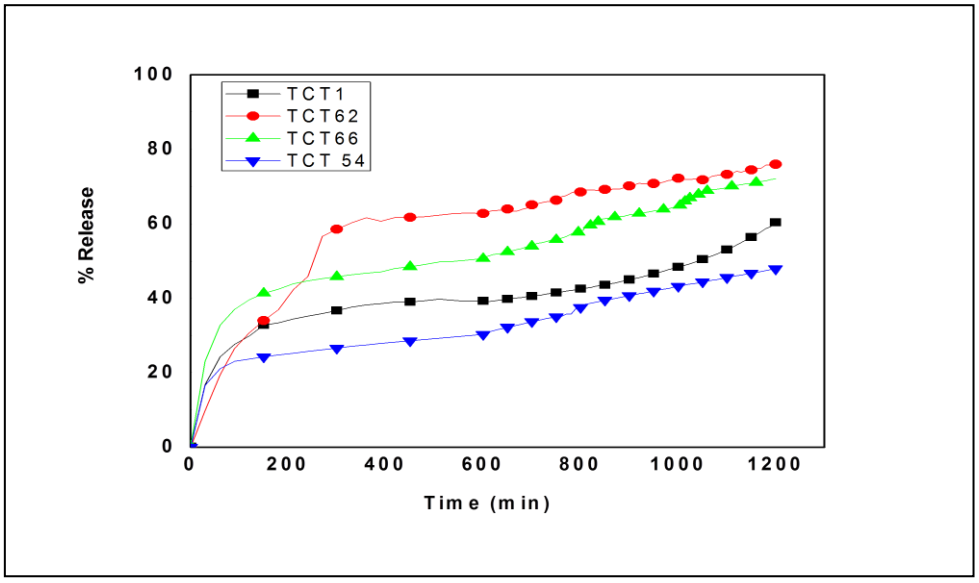

Figure 4.13 In vitro release of theophylline from the prepared nanocomposites (THP-CSNPs).

CHAPTER FIVE

CONCLUSION

- We concluded through this study the possibility of producing nanoparticles of theophylline with chitosan polymer by ionic gelation method with advanced and promising pharmaceutical specifications.
- The software Minitab 18 used in this study shows a full factorial design can be successfully employed in developing THP-CSNPs prepared.
- The prepared nanocomposite is characterized by having sustained release properties with good and stable physical properties, with an acceptable particle nano-size and productive loading efficiency, which was demonstrated by the release of the drug and its stability in the selected nanocomposites.
- We obtained nanoparticles with a wide nano-size range 84 nm_442 nm that provides great prospects for research and the loading efficiency between (70_80%) and stable values of zeta potential. It is concluded that these optimized THP-CSNPs formulation will be an alternative drug delivery system for THP to enhance its bioavailability and the therapeutic index, the results indicated that the tripolyphosphate has the most significant effect on LE, ZP and particle size.

Further works:

- Characterization of the optimized THP-CSNPs nanocomposites using XRD, TGA and TEM.
- The developed formulation will be filled into size 3 gelatin capsules and tested using NGI (Next Generation Impactor) for using to inhalation rout of administration.

- Novel work for study the relationship between release rate as dependent variables with three independent variables (LE%, ZP and particle size).

References

Abouelmagd, S. A., Hyun, H., & Yeo, Y. 2014. Extracellularly activatable nanocarriers for drug delivery to tumors. ***Expert opinion on drug delivery***, 11(10): 1601-1618.

Agnihotri, S. A., Mallikarjuna, N. N., & Aminabhavi, T. M. 2004. Recent advances on chitosan-based micro- and nanoparticles in drug delivery. ***Journal of Controlled Release Journal of Controlled Release***, 100(1): 5-28.

Ahdyani, R., Novitasari, L., Martien, R., & Danarti, R. 2019. Formulation and Characterization of Timolol Maleate-loaded Nanoparticles gel by Ionic Gelation Method Using Chitosan and Sodium Alginate. ***International Journal of Applied Pharmaceutics***, 11(6).

Ahmad, M. 2012. Formulation development and in vitro evaluation of theophylline microcapsules. ***Pakistan Journal of Pharmaceutical Sciences***, 25(1): 15-19.

Aminipour, Z., Kolouei, Z., Tohidi, S., & Bonakdar, S. 2018. Encapsulation of Theophylline in Poly (vinyl alcohol) using Electrospraying Method. ***Journal of Tissues and Materials***, 1(1): 32-39.

Andrei, K. 2011. ***Solubilty and Physical Stability Improvment of Natural Xanthine Derivates***. University of Helsinki Division of Pharmaceutical technology.

Arisoy, S., Ozgun Sayiner, O., Comoglu , T., Onal, D., Atalay, O., & Pehlivanoglu, B. 2020. In vitro and in vivo evaluation of levodopa loaded nanoparticles for nose to brain delivery. ***Pharmaceutical Development and Technology***.

Avadi, M. R., Sadeghi, A. M. M., Mohammadpour, N., Abedin, S., Atyabi, F., Dinarvand, R., & Rafiee-Tehrani, M. 2010. Preparation and characterization of insulin nanoparticles using chitosan and Arabic gum with ionic gelation method. ***Nano Nanomedicine: Nanotechnology, Biology, and Medicine***, 6(1): 58-63.

Bajpai, A. K., Shukla, S. K., Bhanu, S., & Kankane, S. 2008. Responsive polymers in controlled drug delivery. ***Progress in Polymer Science***, 33(11): 1088-1118.

Barnes, P. J. 2013. Theophylline. ***American Journal of Respiratory and Critical Care Medicine***, 188(8): 901-906.

Bhadra, D., Bhadra, S., Jain, S., & Jain, N. K. 2003. A PEGylated dendritic nanoparticulate carrier of fluorouracil. ***International journal of pharmaceutics***, 257(1-2): 1-2.

Calvo, P., Remuñan-López, C., Vila-Jato, J. L., & Alonso, M. J. 1997. Chitosan and Chitosan/Ethylene Oxide-Propylene Oxide Block Copolymer Nanoparticles as Novel Carriers for Proteins and Vaccines. ***Pharmaceutical Research***, 14(10): 1431-1436.

Calvo, P., RemuÞan-Lopez, C., Vila-Jato, J. L., & Alonso, M. J. 1997. Novel Hydrophilic Chitosan-Polyethylene Oxide Nanoparticles as Protein Carriers. ***Journal of Applied Polymer Science***, 63(1): 125-132.

Cauchetier, E., Deniau, M., Fessi, H., Astier, A., & Paul, M. 2003. Atovaquone-loaded nanocapsules: influence of the nature of the polymer on their in vitro characteristics. ***International Journal of Pharmaceutics*** 250(1): 273-281.

Chang, C., Wei, H., Quan, C. Y., Li, Y. Y., Liu, J., Wang, Z. C., Cheng, S. X., Zhang, X. Z., & Zhuo, R. X. 2008. Fabrication of thermosensitive PCL-PNIPAAm-PCL triblock copolymeric micelles for drug delivery. ***Journal of Polymer Science Part A: Polymer Chemistry***, 46(9): 3048-3057.

Chydyrov, P. R. 2007. New mite species of the cohort tarsonemina (Trombidiformes, Acarina) of the fauna of Turkmenistan. **Entomological Review,** 87(6): 767-775.

Crank, J. 2013. ***The mathematics of diffusion***. Oxford: Clarendon.

Dalia A. Elaty, M., Maha K. A, K., & Sameh. S, G. A. D. 2020. Zolmitriptan Brain Targeting via intranasal Route Using Solid Lipid Nanoparticles for Migraine Therapy: Formulation, Characterization, In-vitro and In-vivo Assessment. ***International Journal of Applied Pharmaceutics***, 12(2).

De Jong, W. H., & Borm, J. 2008. Drug delivery and nanoparticles: Applications and hazards. ***International Journal of Nanomedicine***, 3(2): 133-149.

Delan, W. K., Zakaria, M., Elsaadany, B., ElMeshad, A. N., Mamdouh, W., & Fares, A. R. 2020. Formulation of simvastatin chitosan nanoparticles for controlled delivery in bone regeneration: Optimization using Box-Behnken design, stability and in vivo study. ***International Journal of Pharmaceutics***, 577: 119038.

El-Sherbiny, I. M., & Smyth, H. D. C. 2012. Controlled Release Pulmonary Administration of Curcumin Using Swellable Biocompatible Microparticles. ***Molecular Pharmaceutics***, 9(2): 269-280.

Fabritius, H. O., Sachs, C., Triguero, P. R., & Raabe, D. 2009. Influence of Structural Principles on the Mechanics of a Biological Fiber-Based Composite Material with Hierarchical Organization: The Exoskeleton of the Lobster Homarus americanus. ***Advanced Materials -Deerfield Beach then Weinheim-***, 21(4): 391-400.

Feng, Z. Q., Sun, C. G., Zheng, Z. J., Hu, Z. B., Mu, D. Z., & Zhang, W. F. 2015. Optimization of Spray-Drying Conditions and Pharmacodynamics Study of Theophylline/Chitosan/b-Cyclodextrin Microspheres. ***Drying Technology***, 33(1): 55-65.

Fini, A., Cavallari, C., Ospitali, F., & Gonzalez-Rodriguez, M. L. 2011. Theophylline-loaded compritol microspheres prepared by ultrasound-assisted atomization. ***Journal of Pharmaceutical Sci*ences**, 100(2): 743-757.

Fonseca-Santos, B., Satake, C. Y., Calixto, G. M. F., Dos Santos, A. M., & Chorilli, M. 2017. Trans-resveratrol-loaded nonionic lamellar liquid-crystalline systems: structural, rheological, mechanical, textural, and bioadhesive characterization and evaluation of in vivo anti-inflammatory activity. ***International journal of nanomedicine***, 12: 6883-6893.

Fredenberg, S., Wahlgren, M., Reslow, M., & Axelsson, A. 2011. The mechanisms of drug release in poly (lactic-co-glycolic acid)-based drug delivery systems—a review. ***International journal of pharmaceutics***, 415(1-2): 34-52.

Gan, Q., & Wang, T. 2007. Chitosan nanoparticle as protein delivery carrierSystematic examination of fabrication conditions for efficient loading and release. ***Colsub Colloids and Surfaces B: Biointerfaces***, 59(1): 24-34.

Ganesh N, S., C. H. Praveen, K., Birendra, S., & B, K. 2020. Optimization and Characterization of Chitosan-Based Nanoparticles Containing Methylprednisolone Using Box-Behnken Design for the Treatment of Crohn's Disease. ***International Journal of Applied Pharmaceutics***, 12(2).

Gupta, U., Sharma, S., Khan, I., Gothwal, A., Sharma, A. K., Singh, Y., Chourasia, M. K., & Kumar, V. 2017. Enhanced apoptotic and anticancer potential of paclitaxel loaded biodegradable nanoparticles based on chitosan. ***International Journal of Biological Macromolecules***, 98: 810-819.

Hadwiger, L. A. 2013. Plant science review: Multiple effects of chitosan on plant systems: Solid science or hype. ***Plant Science***, 208: 42-49.

Hamman, J. H. 2010. Chitosan based polyelectrolyte complexes as potential carrier materials in drug delivery systems. ***Marine Drugs***, 8(4): 1305-1322.

Herman, E. H., Zhang, J., Hasinoff, B. B., Chadwick, D. P., Clark, J. R., & Ferrans, V. J. 1997. Comparison of the protective effects against chronic doxorubicin cardiotoxicity and the rates of iron (III) displacement reactions of ICRF-187 and other bisdiketopiperazines. ***Cancer Chemotherapy and Pharmacology***, 40(5): 400-408.

Herrlich, S., Spieth, S., Messner, S., & Zengerle, R. 2012. Osmotic micropumps for drug delivery. ***Advanced Drug Delivery Reviews***, 64(14): 1617-1627.

Hofmann, A. 1929. ***On the enzymatic degradation of chitin and Chitosan***. Unpublished Ph.D. thesis, University of Zurich; Zurich, Switzerland.

Hu, Y., Jiang, X., Ding, Y., Ge, H., Yuan, Y., & Yang, C. 2002. Synthesis and characterization of chitosan-poly(acrylic acid) nanoparticles. ***Biomaterials***, 23(15): 3193-3201.

Jain, A., Gupta, Y., & Jain, S. K. 2007. Perspectives of biodegradable natural polysaccharides for site-specific drug delivery to the colon. ***Journal of pharmacy & pharmaceutical sciences***, 10(1): 86-128.

Jayakumar, R., Chennazhi, K. P., Muzzarelli, R. A. A., Tamura, H., Nair, S. V., & Selvamurugan, N. 2010. Chitosan conjugated DNA nanoparticles in gene therapy. ***Carbohydrate Polymers***, 79(1): 1-8.

Jeong, Y. I., Jin, S. G., Kim, I. Y., Pei, J., Wen, M., Jung, T. Y., Moon, K. S., & Jung, S. 2010. Doxorubicin-incorporated nanoparticles composed of poly(ethylene glycol)-grafted carboxymethyl chitosan and antitumor activity against glioma cells in vitro. ***Colloids and Surfaces B: Biointerfaces***, 79(1): 149-155.

Katas, H., & Alpar, H. O. 2006. Development and characterisation of chitosan nanoparticles for siRNA delivery. ***Journal of Controlled Release,*** 115(2): 216-225.

Karimi, M., Avci, P., Ahi, M., Gazori, T., R., M., Hamblin, & Naderi-Manesh, H. 2013. Evaluation of Chitosan-Tripolyphosphate Nanoparticles as a p-shRNA Delivery Vector: Formulation, Optimization and Cellular Uptake Study. ***Journal of Nanopharmaceutics and Drug Deliv*****ery**, 1(1): 266-278.

Kawashima, Y. 2001. Preface nanoparticulate systems for improved drug delivery. ***Advanced Drug Delivery Rev*****iews**, 47(1): 1-2.

Kean, T., & Thanou, M. 2010. Biodegradation, biodistribution and toxicity of chitosan. ***Advanced Drug Delivery Reviews***, 62(1): 3-11.

Khor, E., & Lim, L. Y. 2003. Implantable applications of chitin and chitosan. ***Biomaterials***, 24(13): 2339-2349.

Kiran, B., Shadab, K., & Ghazala, M. 2020. Topical Anti-Psoriatic Nanoparticulate Drug Delivery System. ***International Journal of Applied Pharmaceutics***, 12(2).

Kompella, U. B., Bandi, N., & Ayalasomayajula, S. P. 2003. Subconjunctival Nano- and Microparticles Sustain Retinal Delivery of Budesonide, a Corticosteroid Capable of Inhibiting VEGF Expression. ***Investigative Opthalmology & Visual Science***, 44(3): 1192.

Kramarenko, E. Y., Khokhlov, A. R., & Reineker, P. 2006. Stoichiometric polyelectrolyte complexes of ionic block copolymers and oppositely charged polyions. ***The Journal of chemical physics***, 125(19).

Kukreja, A., Chopra, P., Aggarwal, A., Khanna, P. J. I. J. o. M., & Optimization. 2011. Application of full factorial design for optimization of feed rate of stationary hook hopper. 1(3): 205.

Langer, R., & Peppas, N. 1983. Chemical and Physical Structure of Polymers as Carriers for Controlled Release of Bioactive Agents: A Review. ***Journal of Macromolecular Science, Part C Journal of Macromolecular Science, Part C***, 23(1): 61-126.

Lee, J. H., & Yeo, Y. 2015. Controlled Drug Release from Pharmaceutical Nanocarriers. ***Chemical engineering science***, 125: 75-84.

Lee, S. H., Mok, H., Lee, Y., & Park, T. G. 2011. Self-assembled siRNA-PLGA conjugate micelles for gene silencing. ***Journal of Controlled Release***, 152(1): 152-158.

Li, W., Li, J., Gao, J., Li, B., Xia, Y., Meng, Y., Yu, Y., Chen, H., Dai, J., Wang, H., & Guo, Y. 2011. The fine-tuning of thermosensitive and degradable polymer micelles for enhancing intracellular uptake and drug release in tumors. ***Biomaterials***, 32(15): 3832-3844.

Lin, C. C., & Metters, A. T. 2006. Hydrogels in controlled release formulations: Network design and mathematical modeling. ***Advanced Drug Delivery Reviews***, 58(12-13): 1379-1408.

Mahdavinia, G. R., Mosallanezhad, A., Soleymani, M., & Sabzi, M. 2017. Magnetic- and pH-responsive κ-carrageenan/chitosan complexes for controlled release of methotrexate anticancer drug. ***International Journal of Biological Macromolecule,*** 97: 209-217.

Mansouri, S., Cuie, Y., Winnik, F., Shi, Q., Lavigne, P., Benderdour, M., Beaumont, E., & Fernandes, J. C. 2006. Characterization of folate-chitosan-DNA nanoparticles for gene therapy. ***Biomaterials***, 27(9): 2060-2065.

Medina, S. H., Chevliakov, M. V., Tiruchinapally, G., Durmaz, Y. Y., Kuruvilla, S. P., & Elsayed, M. E. 2013. Enzyme-activated nanoconjugates for tunable release of doxorubicin in hepatic cancer cells. ***Biomaterials***, 34(19): 4655-4666.

Min, K. H., Kim, J. H., Bae, S. M., Shin, H., Kim, M. S., Park, S., Lee, H., Park, R. W., Kim, I. S., Kim, K., Kwon, I. C., Jeong, S. Y., & Lee, D. S. 2010. Tumoral acidic pH-responsive MPEG-poly(beta-amino ester) polymeric micelles for cancer targeting therapy. ***Journal of Controlled Release***, 144(2): 259-266.

Mohanraj, V. J., & Chen, Y. 2006. Nanoparticles - A review. ***Tropical Journal of Pharmaceutical Research***(5): 561-573.

Mourya, V. K., & Inamdar, N. N. 2008. Chitosan-modifications and applications: Opportunities galore. ***Reactive and Functional Polymers***, 68(6): 1013-1051.

Muzzarelli, R. A. A., & Muzzarelli, C. 2005. Chitosan Chemistry: Relevance to the Biomedical Sciences. ***Advances in Polymer Science***, 186: 151-210.

Naahidi, S., Jafari, M., Edalat, F., Raymond, K., Khademhosseini, A., & Chen, P. 2013. Biocompatibility of engineered nanoparticles for drug delivery. ***Journal of Controlled Release***, 166(2): 182-194.

Nallamuthu, I., Devi, A., & Khanum, F. 2015. Chlorogenic acid loaded chitosan nanoparticles with sustained release property, retained antioxidant activity and enhanced bioavailability. ***Asian Journal of Pharmaceutical Sciences***, 10(3): 203-211.

Oprea, A.-M., Nistor, M.-T., Popa, M. I., Lupusoru, C. E., & Vasile, C. 2012. In vitro and in vivo theophylline release from cellulose/chondroitin sulfate hydrogels. ***Carbohydrate Polymers***, 90(1): 127-133.

Panta, A., & Negiab, J. S. 2018. Novel controlled ionic gelation strategy for chitosan nanoparticles preparation using TPP-β-CD inclusion complexv. ***European Journal of Pharmaceutical Sciences***,112: 180-185.

Pattanayek, S., & Puranik, S. B. 2018. Development and evaluation of ketoprofen loaded particles. ***International journal of pharmacy and pharmaceutical research,***11(3): 225-237.

Peppas, N. A., Bures, P., Leobandung, W., & Ichikawa, H. 2000. Hydrogels in pharmaceutical formulations. ***European Journal of Pharmaceutics and Biopharmaceutics***, 50(1): 27-46.

Prabaharan, M., Grailer, J. J., Pilla, S., Steeber, D. A., & Gong, S. 2009. Amphiphilic multi-arm-block copolymer conjugated with doxorubicin via pH-sensitive hydrazone bond for tumor-targeted drug delivery. ***Biomaterials***, 30(29): 5757-5766.

Ravi Kumar, M. N. V. 2000. A review of chitin and chitosan applications. ***Reactive and Functional Polymers Reactive and Functional Polymers***, 46(1): 1-27.

Ravi Kumar, M. N. V., Bakowsky, U., & Lehr, C. M. 2004. Preparation and characterization of cationic PLGA nanospheres as DNA carriers. ***Biomaterials***, 25(10): 1771-1777.

Reverchon, E., & Adami, R. 2006. Nanomaterials and supercritical fluids. ***The Journal of Supercritical Fluids***, 37(1): 1-22.

Rolland, J. P., Maynor, B. W., Euliss, L. E., Exner, A. E., Denison, G. M., & DeSimone, J. M. 2005. Direct Fabrication and Harvesting of Monodisperse, Shape-Specific Nanobiomaterials. ***Journal of the American Chemical Society***, 127(28): 10096-10100.

Salem, H., ME., A., Abo Eid, K., & Sharaf, M. 2011. Nanosized rods agglomerates as a new approach for formulation of a dry powder inhaler. ***International Journal of Nanomedicine***, 6: 311-320.

Shi, X. Y., Fan, X. G., & Original, L. 2002. Advances in nanoparticle system for deliverying drugs across the biological barriers. ***Journal of China Pharmaceutical University.***, 33: 169-172.

Shur, B. 2007. ***Prepartion of chitosan and its use in defluorination of water***. Unpublished Doctoral dissertation.

Siegel, R. A., & Rathbone, M. J. 2012. ***Fundamentals and applications of controlled release drug delivery.***: Springer; New York.

Solunke S.R., Borge, R. U., Murthy, K., Deshmukh, T. M., & Shete5, V. R. 2019. Formulation and Evaluation of Gliclazide Nanosponges. ***International Journal of Applied Pharmaceutics***, 11(6): 181-189.

Song, C. W., Griffin, R., & Park, H. J. 2006. Influence of Tumor pH on Therapeutic Response, ***Cancer Drug Resistance***.

Talelli, M., Iman, M., Varkouhi, A. K., Rijcken, C. J., Schiffelers, R. M., Etrych, T., Ulbrich, K., van Nostrum, C. F., Lammers, T., Storm, G., & Hennink, W. E. 2010. Core-crosslinked polymeric micelles with controlled release of covalently entrapped doxorubicin. ***Biomaterials***, 31(30): 7797-7804.

Thomas, D., Nair, V. V., Latha, M. S., & Thomas, K. K. 2019. Theoretical and experimental studies on theophylline release from hydrophilic alginate nanoparticles. ***Future Journal of Pharmaceutical Sciences***, 5(1).

Tığlı Aydın, R. S., & Pulat, M. 2012. 5-Fluorouracil Encapsulated Chitosan Nanoparticles for pH-Stimulated Drug Delivery: Evaluation of Controlled Release Kinetics. ***Journal of Nanomaterials***, 2012: 313961.

Vyas A, Saraf S, Saraf S. Encapsulation of cyclodextrin complexed simvastatin in chitosan nanocarriers: A novel technique for oral delivery. ***Journal of Inclusion Phenomena and Macrocyclic Chemistry***. 2010;66:251.

Weber, C., Coester, C., Kreuter, J., & Langer, K. 2000. Desolvation process and surface characterisation of protein nanoparticles. ***International journal of pharmaceutics.***, 194(1): 91.

Yancheva, E., Paneva, D., Maximova, V., Mespouille, L., Dubois, P., Manolova, N., & Rashkov, I. 2007. Polyelectrolyte Complexes between (Cross-linked) N-Carboxyethylchitosan and (Quaternized) Poly[2-(dimethylamino)ethyl methacrylate]: Preparation, Characterization, and Antibacterial Properties. ***Biomacromolecules***, 8(3): 976-984.

Yih, T. C., & Al-Fandi, M. 2006. Engineered nanoparticles as precise drug delivery systems. ***Journal of Cellular Biochemistry***, 97(6): 1184-1190.

Yuba, E., Harada, A., Sakanishi, Y., Watarai, S., & Kono, K. 2013. A liposome-based antigen delivery system using pH-sensitive fusogenic polymers for cancer immunotherapy. ***Biomaterials***, 34(12): 3042-3052.

Zhao, H., Wei, Y., Qiao, R., Zhu, C., Zheng, Z., Ling, M., Jia, Z., Bai, Y., Fu, Y., Lei, J., Song, X., Battaglia, V. S., Yang, W., Messersmith, P. B., & Liu, G. 2015. Conductive Polymer Binder for High-Tap-Density Nanosilicon Material for Lithium-Ion Battery Negative Electrode Application. ***Nano letters***, 15(12): 7927-7932.

Zhiyang Du, Jingbo Liu, Ting Zhang, Yiding Yu, Yan Zhang, Jinxing Zhai, Haitao Huang, Shibiao Wei, Long Ding, Boqun Liu. ***Journal Data in Brief,*** Volume 28, February 2020, 04841

Zu, C., Yu, Y., Yu, C., Li, Y., Sun, R., Chaurasiya, B., Tang, B., Chen, D., Tu, J., & Shen, Y. 2020. Highly loaded deoxypodophyllotoxin nano-formulation delivered by methoxy polyethylene glycol-block-poly (D,L-lactide) micelles for efficient cancer therapy. ***Drug Delivery***, 27(1): 248-257.

APPENDICES

APPENDIX A: Analysis of THP drug.

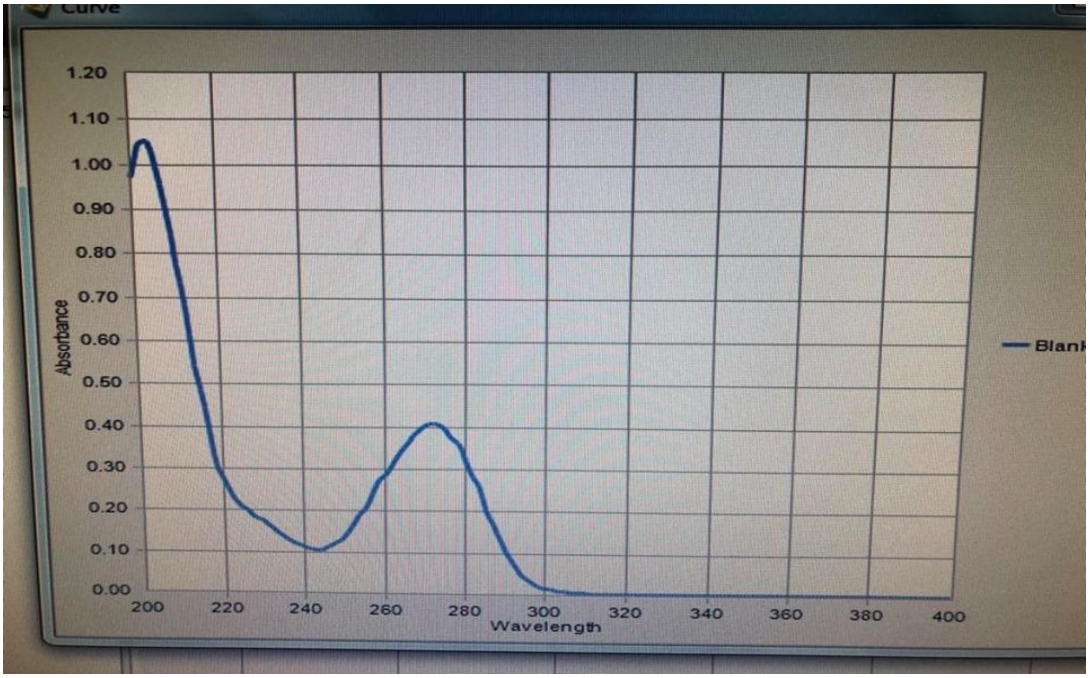

APPENDIX B: Standard calibration curve of THP drug.

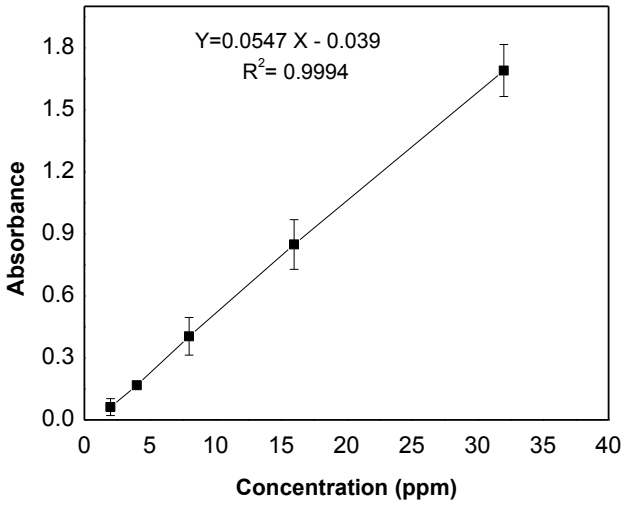

APPENDIX C: Analysis of CSNPs.

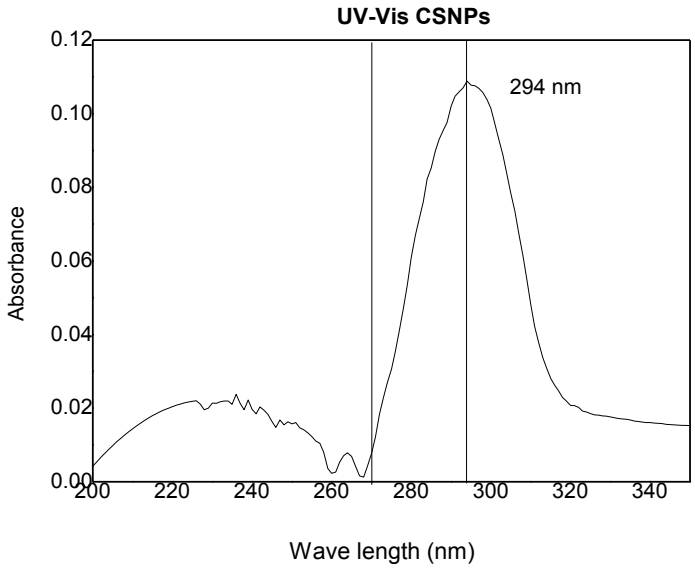

APPENDIX D: Kinetic study in UV-vis spectrophotometer

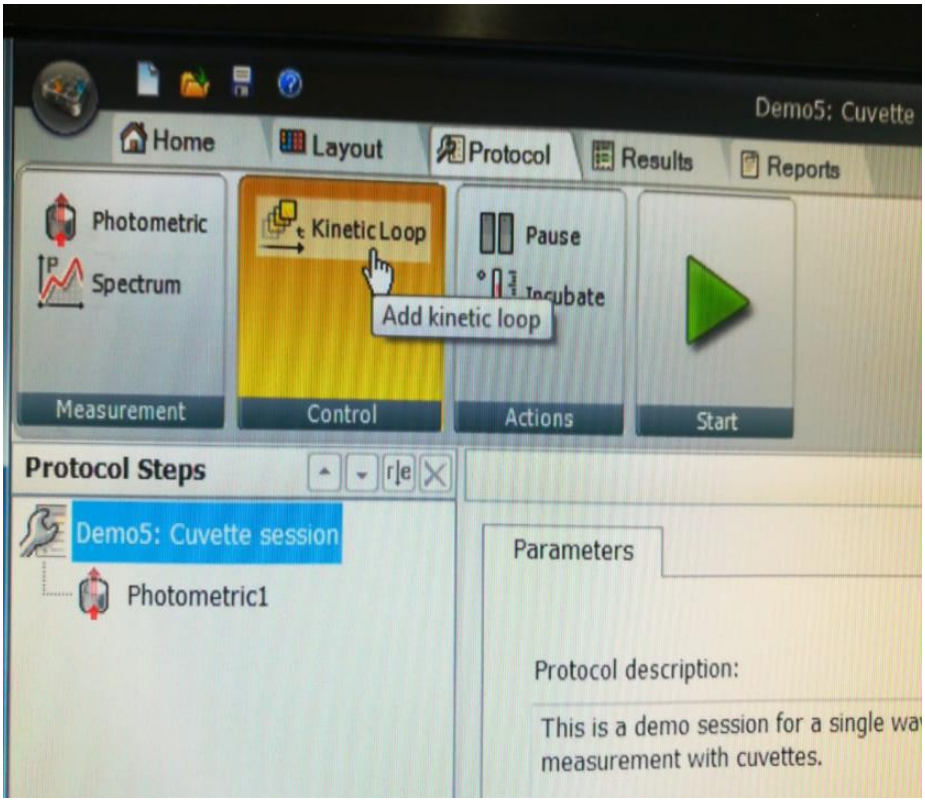

الخلاصة

الهدف من هذه الدراسة هو تطبيق استخدام الجسيمات النانوية كناقلات أدوية .تضمنت الدراسة تحضير جزيئات نانوية من دواء الثايوفلين للتغلب على مشكلة جرعة الثايوفلين وتحسين خصائص الدواء.تم تحضير حبيبات نانوية الثايوفلين مع الشيتوزان بكميات مختلفة من الشيتوزان (٥٠ و٧٥ و ١٠٠ و ١٥٠ ملغم).كذلك كميات مختلفة من الترايبوليفوسفيت (٢٥ و ٥٠ و ٧٥ و١٠٠ و ٢٠٠ ملغم) مع كمية محددة من الثايوفلين وهي ١٠٠ ملغم.

ودرجة حامضية بدالة الاس الهيدروجيني (٤ و ٥ و ٦ و ٦,٥) .يتم تمييز المنتج النهائي للمركبات النانوية باستخدام الاشعة تحت الحمراء لتمييز الثايوفلين الحرة والمحملة بالشيتوزان لتقدير المجاميع الفعالة للمركب .تم استخدام البرنامج التحليلي الاحصائي مينيتاب ١٨حيث تم تحليل النتائج باستخدام التحليلات الرسومية مثل المخططات السطحية والكونتورية مع مخطط باريتو و رسومات الاحتمالية ورسومات المتبقيات وغيرها.المتغيرات المستقلة كانت هي كمية الشيتوزان و الترايبوليفوسفيت و درجة الحامضية اما المتغيرات التابعة وغير المستقلة فهي حجم الحبيبات النانوية وجهد زيتا وكفاءة تحميل الدواء على البوليمر.من خلال التجارب تمكنا من الحصول على مركبات نانوية من الثايوفلين والشيتوزان وفي نطاق حجم مقبول وبمواصفات عالية والتي نجحت في حمل الدواء وحفظه ومن ثم تحرره في الاطلاق المختبري بشكل مديد الوقت .